To the Graduate Council:

I am submitting herewith a thesis written by Steven Alan Spraggins entitled "Deformation History of a Foreland Thrust Belt in a Recess: An Example from the Roanoke Recess, Appalachians, USA." I have examined the final copy of this thesis for form and content and recommend that it be accepted in partial fulfillment of the requirements for the degree of Master of Science, with a major in Geology.

William M. Dunne

William M. Dunne, Major Professor

We have read this thesis and recommend its acceptance:

Robert D. Hatcher Jr.

Robert D. Hatcher, Jr.

Kenneth R. Walker

Kenneth R. Walker

Accepted for the Council:

Carolyn Minkel

Associate Vice Chancellor and Dean of The Graduate School

DEFORMATION HISTORY OF A FORELAND THRUST BELT IN A RECESS: AN EXAMPLE FROM THE ROANOKE RECESS, APPALACHIANS, USA

A Thesis
Presented for the
Master of Science
Degree
The University of Tennessee, Knoxville

Steven Alan Spraggins
December 1999

ACKNOWLEDGEMENTS

I appreciate the work of Bill Dunne, Kevin Smart and Brent Couzens in thinking up this project and ‘paving the way’ for me. I owe Bill a debt of gratitude for his hard work, encouragement and calcite twin expertise. I am grateful to my thesis committee, Bill Dunne, Bob Hatcher and Ken Walker, for their guidance and useful comments. I would like to thank Southeastern Geological Society of America and Sigma Xi for their generous assistance in financial support.

I owe a lot of thanks to my undergraduate professors at the University of Arkansas at Little Rock, Phil Kehler, Jeff Connelly, and Don Owens, for leading me toward graduate studies at the University of Tennessee, and initiating the internship that lead to my current job at Johnson Space Center.

Lastly, I am grateful to have such a loving and supportive family, Jerry, Kathy, Mike, Janis and my wonderful wife Susan. Without their help and encouragement I could never have made it this far.

ABSTRACT

The purposes of this thesis are to investigate the kinematic evolution of the Appalachian foreland thrust belt around the Roanoke recess; to compare the kinematic evolution of a recess to an adjacent salient to see if they deformed in a manner that mirrors their geometry; and to investigate the role of blind thrusts through the deformation of the recess. The key results are: (1) deformation around the recess was continuous as opposed to 'two-step', initiated to the southwest and migrated northeastward while shortening directions rotated counterclockwise from N-S to almost E-W; (2) the recess did not deform as a simple inverse to the Pennsylvania salient; and (3) shortening magnitudes within the recess are sufficient to necessitate blind thrusting through the deformation history.

The study area is located on the Appalachian Plateau in the inner arc of the Roanoke recess where map-scale structures of the central and southern Appalachian foreland thrust belt meet. The stratigraphic unit for the study is the Mississippian Greenbrier Group that is well exposed and contains both abundant stylolitic cleavage and other strain markers for analysis. The primary methods for achieving the purposes of the thesis are: (1) construction of a cross section across the Plateau in the inner arc of the recess to integrate shortening components from map to microscale; (2) chronicling of the abundance and geometry of outcrop-scale folds and faults; (3) analysis of stylolitic cleavage for shortening directions, magnitudes and sequences; (4) analysis of the finite strain

in cleavage microlithons using framework grains in grainstones as strain markers; and (5) analysis of calcite-twin strains to resolve deformation sequences and the contribution of volume-constant deformation to the kinematic behavior.

TABLE OF CONTENTS

LIST OF TABLES

LIST OF FIGURES

1. Introduction

The primary objective of this thesis is to evaluate the kinematic evolution of a thrust belt at a recess, using the timing and deformation contributions of structures in the interior of the recess. A recess is a map-view curve in an orogenic belt that is concave toward the craton, while a salient is a convex curve toward the craton defined by lateral variations in structural trend (Fig.1).

An important kinematic issue for the evolution of these curves is the role of rotation in their formation. These curves may be oroclines that result from rotation by many different tectonic processes: oblique intersection of orogens, interaction of an orogen with obstacles in the foreland, horizontal rotation of crustal blocks, irregular continental margins, lateral variation in pre-deformational basin stratigraphy, lateral variation in orogenic taper, and interaction of an orogen with a pre-existing strike-slip fault (Carey, 1955; Ries and Shackleton, 1976; Thomas, 1977; Marshak and Tabor, 1989; Ferrill and Groshong, 1993a; Marshak and Flottmannn, 1996; Gray and Stamatakos, 1998; Hindle and Burkhard, 1999; Macedo and Marshak, 1999). Yet, many curved belts are not produced by rotation. They are nonrotational orogenic arcs, which by definition are not oroclines (Ries and Shackleton, 1976; Marshak, 1988).

A variety of data types are used to examine whether salient development has been rotational or nonrotational: variations in magnetic declination, structural geometry, deformation magnitudes, transport/stretching directions, and deformation sequences (Carey, 1955; Ries and Shackleton, 1976; Kellogg, 1980; Schwartz and Van der Voo, 1983; Globerman and Coe, 1984; Geissman

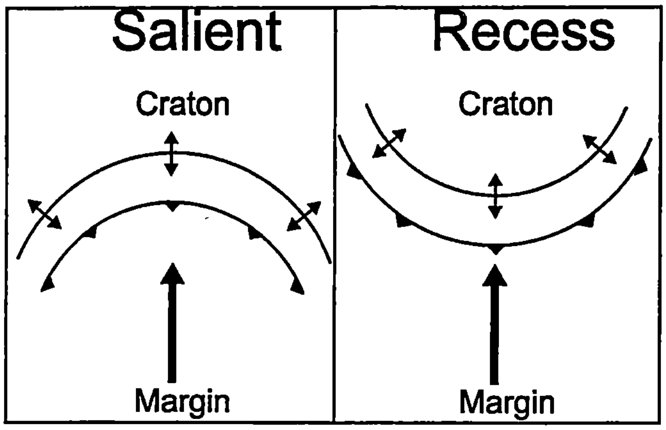

Fig. 1. Salient and recess showing transport direction (arrow) and structural geometry relative to the craton and continental margin.

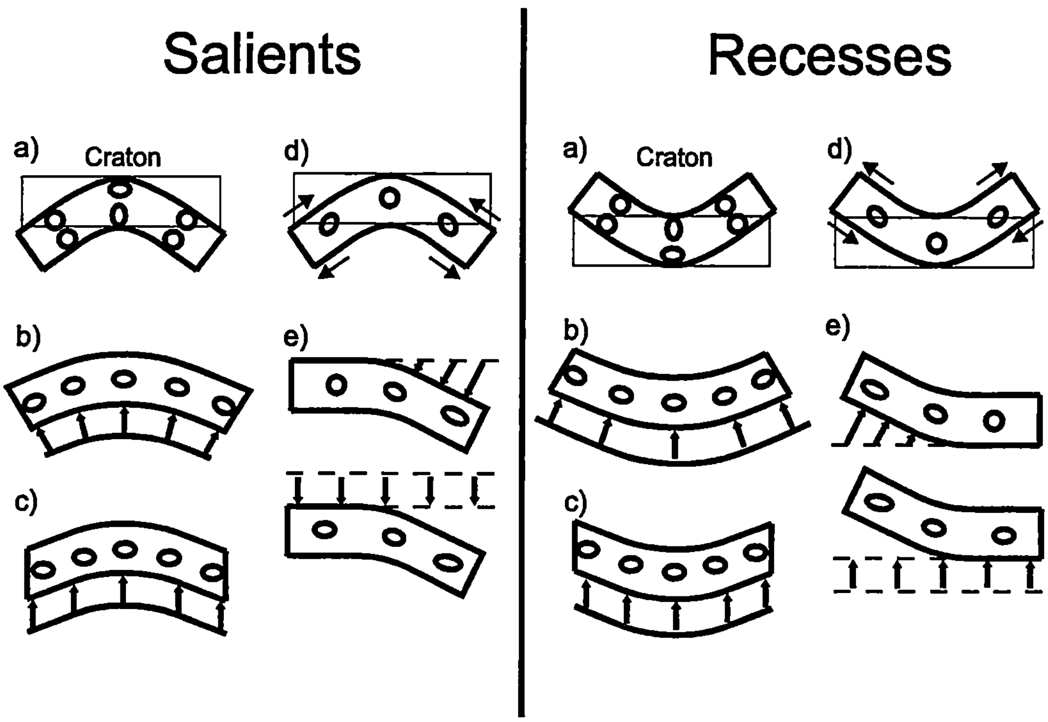

Fig. 2. Kinematic models for formation of salients and recesses (modified from Marshak,1988; Ferril, 1993a). Circles and ellipses show schematic strain distributions. (a) Bending, (b) Radial (salient) and centripetal (recess) displacement, (c) parallel and equal displacements on a pre-existing curve, (d) curve-parallel simple shear, and (e) two-step history (thin-lined rectangles and dashed lines represent undeformed reference features).

et al., 1984; Choukroune et al., 1986; Ferrill and Groshong, 1993a; Marshak and Flottmann, 1996; Hindle and Burkhard, 1999). These data provide tests for the predictions of kinematic models for salient development that include: bending, radial thrusting, parallel displacement paths, curve-parallel simple shear and two-step overprint (Fig. 2). For example, Marshak (1988) emphasized the importance of strain parallel to strike for determining the causes of both oroclines and nonrotational arcs. Ferrill and Groshong (1993a) also used predictions of strain magnitudes to test the applicability of different models for salients to a field example.

Kinematic models for salients do provide a starting point for interpreting recess development by considering the inverse cases (Fig. 2). The problem of recess formation has not received nearly as much attention as salient development (Fig. 2). Marshak and Tabor (1989) did investigate the origin of the New York recess and found a two-step overlapping deformation history that rotated structures at an intersection orocline. Thus, this deformation history for the recess could be described in terms of the simple models for salients (Fig. 2). The first objective of the present study will be to analyze the deformation in the Roanoke recess to determine whether it too deformed in a manner comparable to a salient.

A second objective of this thesis relates to better understanding the evolution of the Roanoke recess at the junction of the southern and central Appalachians (Fig. 3). At this recess, foreland thrusts trending 060° of the

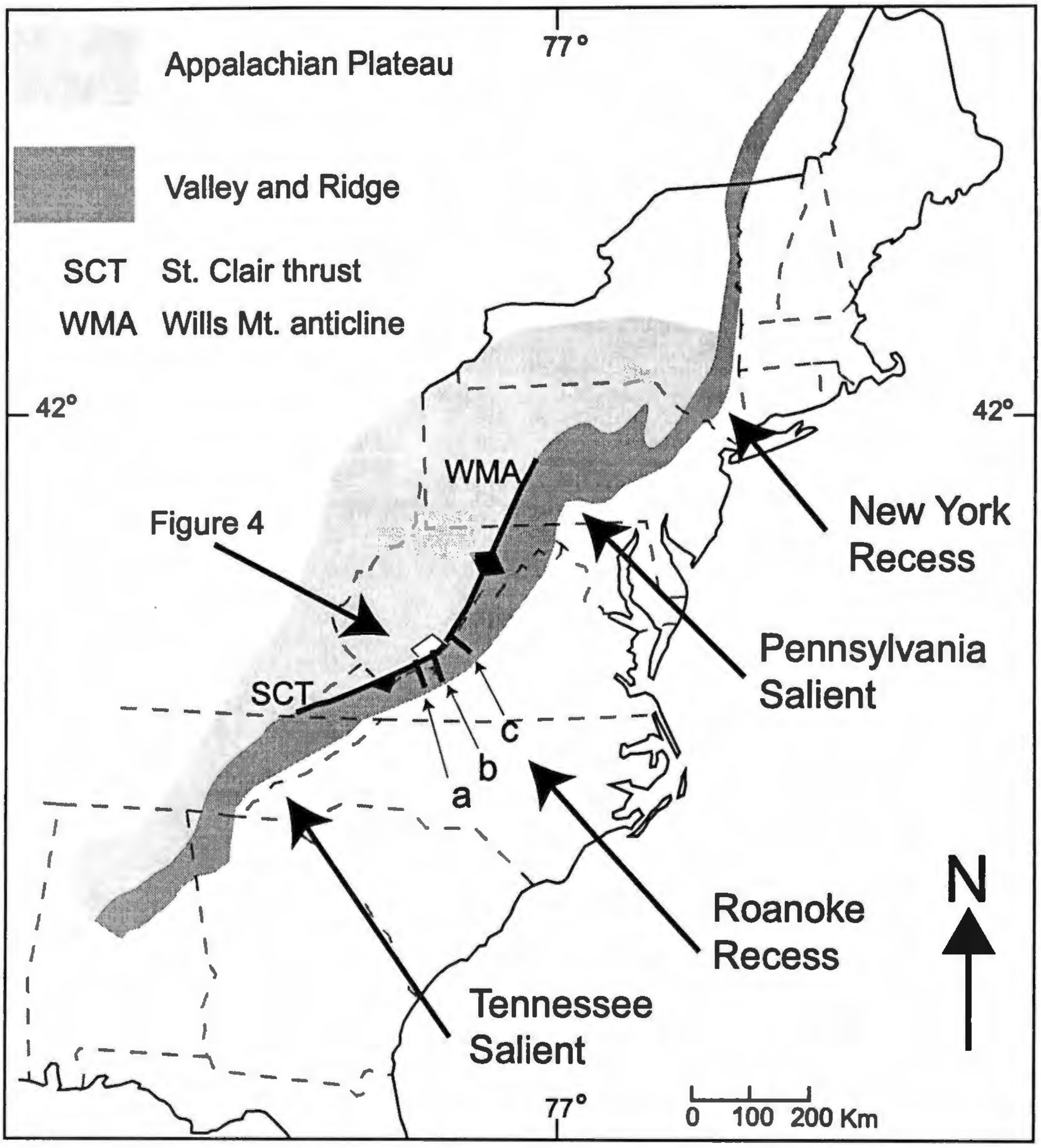

Fig. 3. Location of Roanoke recess with respect to the salients and the other recess of the Appalachians. Also shown is the coverage area for figure 4 and the section locations for figure 5.

southern Appalachians meet surface macrofolds above blind thrust duplexes trending 025° of the central Appalachians. The structures intersect forming a curve around a pre-existing promontory (Thomas, 1977; Hatcher et al., 1989). The prevailing view is that these structures formed during the Alleghanian orogeny but that the southern structures are older (Rodgers, 1970; Dean et al., 1988). The evidence for this interpretation is that the youngest deformed strata in the southern Appalachian foreland are older than in the central Appalachian foreland (Rodgers, 1970); map-scale fold interference in the transition zone shows central overprinting southern (Bick, 1986); and cleavages related to southern Appalachian shortening are contained in the limbs of folds with central Appalachian trends (Dean et al., 1988). Recently, Whitaker and Bartholomew (1999) have disagreed with this view based on strain data from the overturned limb of a fold with a southern Appalachian trend, which they believe to indicate the small-scale deformation of central Appalachian origin preceded large-scale southern Appalachian deformation. As a result, issues remain for the Roanoke recess: (1) which if either of southern and central Appalachian deformation events occurred first at the recess; (2) are models not involving two-step histories more applicable; and (3) how does the recess deformation history account for the interaction between blind central Appalachian duplexes and possibly emergent southern Appalachian thrusts, which have large displacements and are laterally continuous.

2. Geological Setting and Previous Work

The study area is located in the Appalachian Plateau in the inner arc of the Roanoke recess (Fig. 3, 4, 5). To the southeast, the Plateau is bounded structurally by the St. Clair thrust and the footwall Glen Lyn syncline of southern Appalachian origin (Rodgers, 1970). To the east, it is bounded by the Wills Mountain anticline, which is over the blind Wills Mountain duplex of central Appalachian origin (Perry, 1978; Wilson and Shumaker, 1992; Dunne, 1996). To the northwest beyond the study area, the Plateau is bounded by the North American craton (Muehlberger, 1992).

2.1. Target stratigraphic unit

This study uses limestones within the Upper Mississippian Greenbrier Group (Reger and Price, 1926; Ogden, 1976; Skinner, 1979) (Fig. 5) because: (1) limestone is probably the most effective sedimentary rock for investigating low-intensity meso- and microscale deformation (Cloos, 1947; Groshong, 1972; Marshak and Engelder, 1985; Schmid et al., 1987; Groshong, 1988; Protzman and Mitra, 1990; Smart et al., 1997); (2) calcite deforms by a variety of deformation mechanisms that yield many different structures such as twinned grains, overgrowths, calcite fibers, stylolites and cleavage (Fig. 6), providing partial and finite strains (Groshong; 1972; Powell, 1979; Marshak and Engelder, 1985; Meyer and Dunne, 1990); (3) the unit has abundant outcrops in the inner arc of the recess. The unit has an average thickness of about 340 m in the study area, consists of six major formations (Fig. 7) and is conformably overlain by the

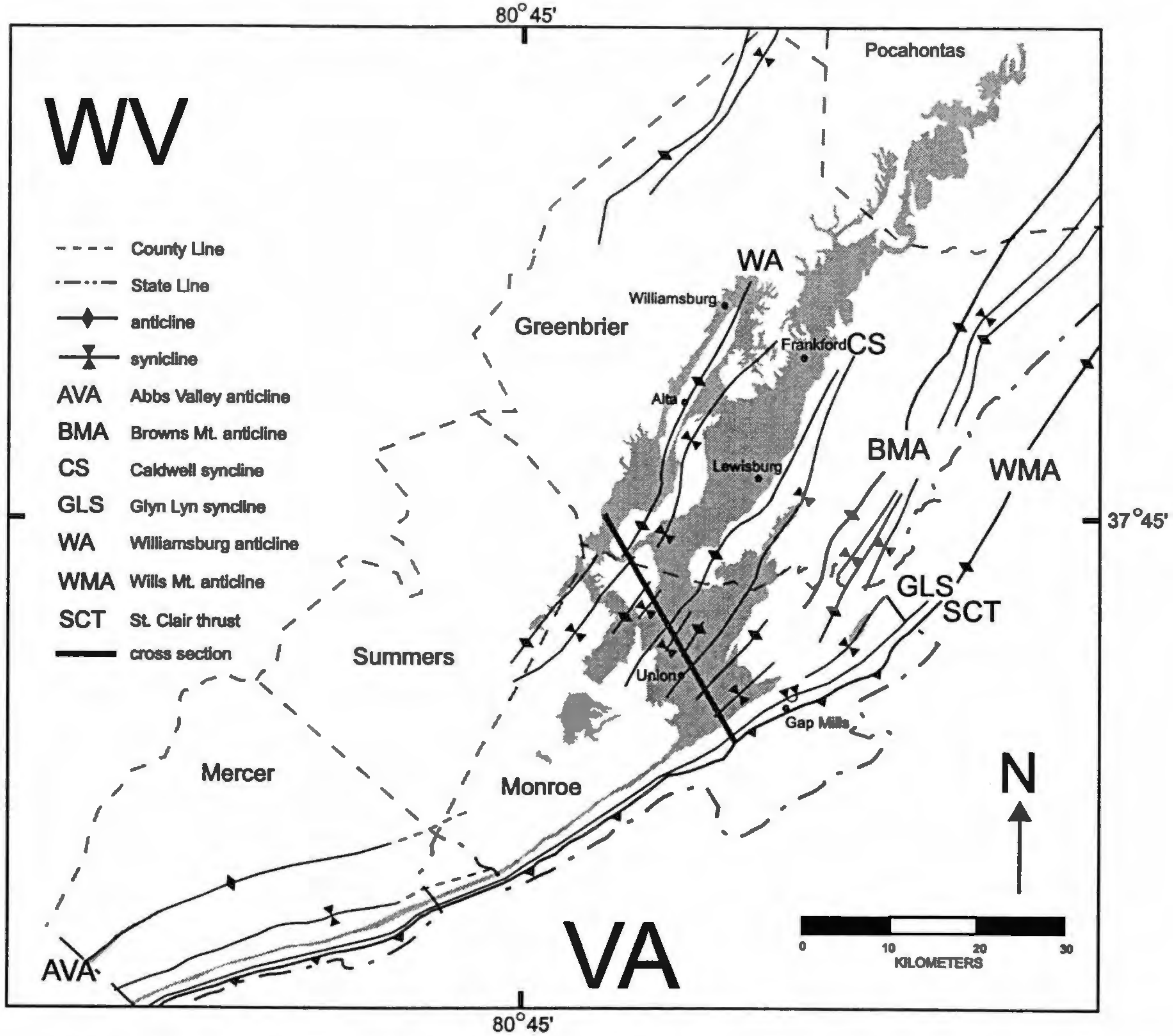

Fig. 4. Greenbrier outcrop belt (gray) modified from Cardwell et al. (1968), cross section line (Figure 7) and major structures from Mercer to Pocohontas County, West Virginia (see Figure 3 for location).

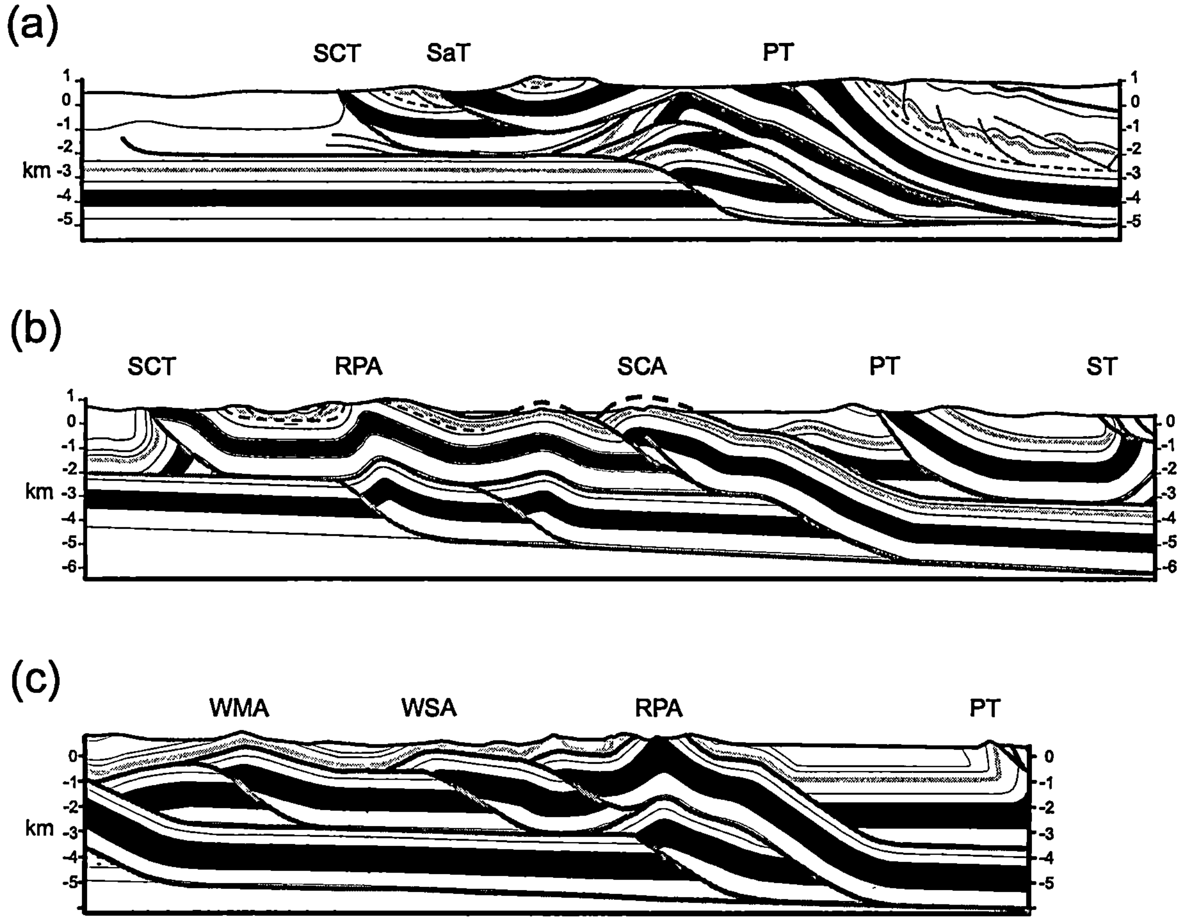

Fig. 5. (a) Cross section for southern Appalachians (Kulander and Dean, 1986). (b) Cross section for transitional region (Onasch and Dunne, 1993). (c) Cross section for central Appalachians (Couzens and Dunne, 1994). Section locations in Fig. 4. Solid black unit is the Cambro-Ordovician Knox Group or stratigraphic equivalent. NT- Narrows thrust; PT-Pulaski thrust; RPA-Rich Patch anticline; SCA-Sinking Creek anticline; SaT-Saltville thrust; ST-Salem thrust; WMA-Wills Mountain anticline; WSA-Warm Springs anticline.

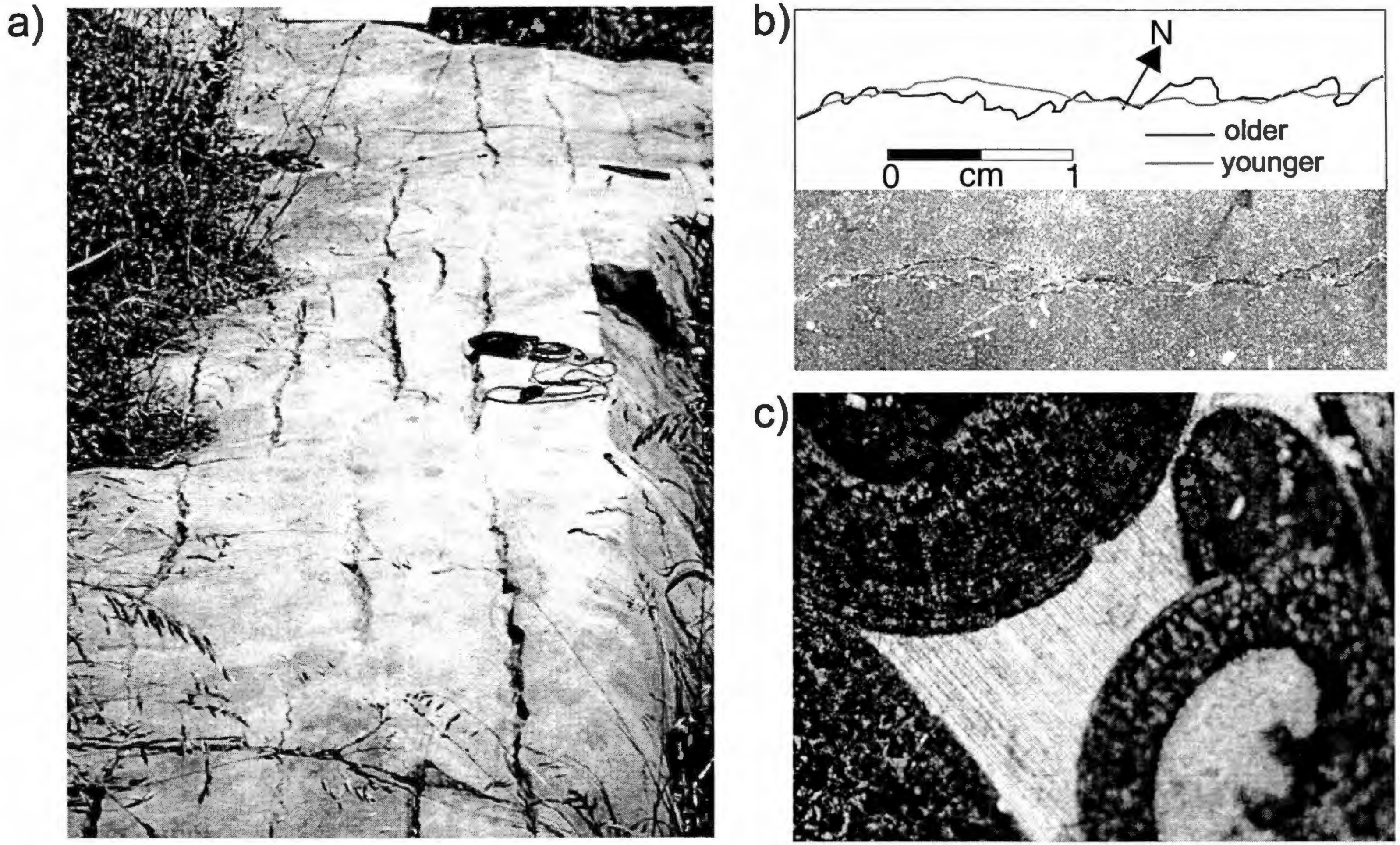

Fig. 6. (a) Greenbrier bedding pavement with bed-normal stylolitic cleavage (Silva Ranger (TM) for scale). (b) Cross-cutting stylolites from station J1 with interpretation above photograph. (c) Twinned calcite cement grain between ooid grains with evidence for grain-to-grain dissolution (photo 1 mm wide).

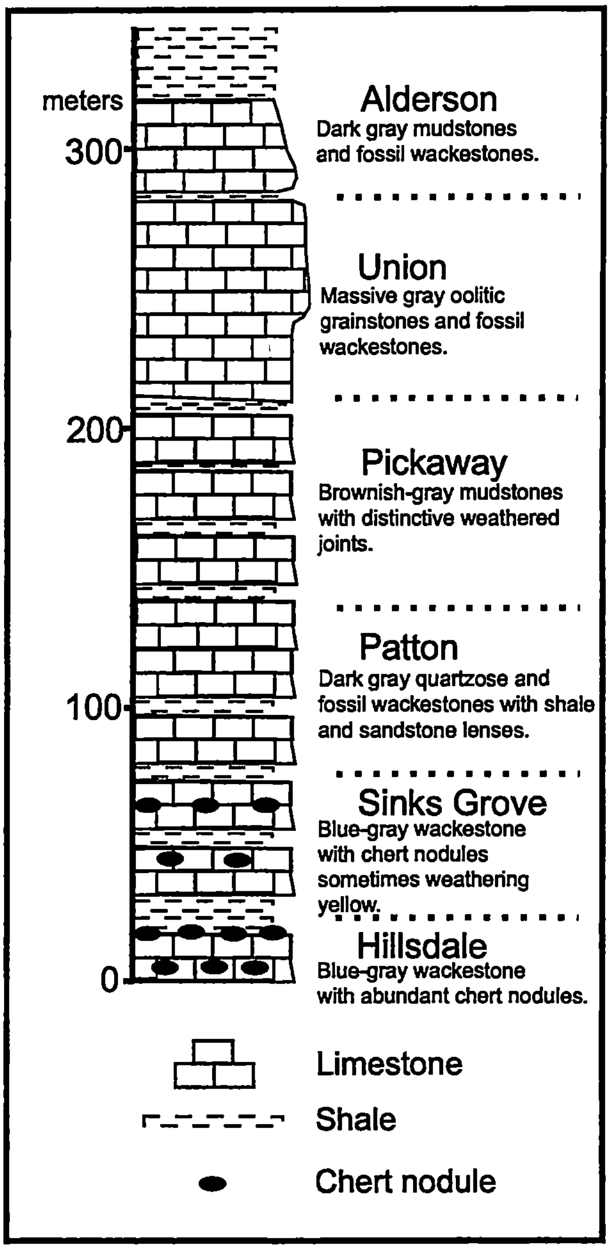

Fig. 7. Stratigraphic column for the Mississippian Greenbrier Group in Monroe County (modified from Reger and Price, 1926; Ogden, 1976; Skinner, 1979).

Mississippian Mauch Chunk Group, and underlain by the Mississippian MacCrady Formation. The primary lithology for this investigation is oolitic grainstone (Dunham, 1962), although some stylolitic shortening values were measured in packstones. This sampling restriction was used to eliminate lithology as a variable when analyzing structural suites in different locations.

2.2. Blind thrusts and the transition from the southern to central Appalachians

The northward transition from the southern to central Appalachians is marked by several changes in structural style (Rodgers, 1970; Kulander and Dean, 1986; Woodward, 1985; Onasch and Dunne, 1993). The structural trend changes from 055°-060° to 025°-030°. Presently emergent thrusts mostly with maximum displacements exceeding 20 km give way to map-scale folds above blind duplexes with displacements up to 20 km. Thrust sheets of rocks ranging in age from Cambrian to Mississippian give way to horses of Cambrian to Middle Ordovician rocks that underlie a decoupled roof sequence of Middle Ordovician to Mississippian rocks (Fig. 5). All of these changes occur in the Valley and Ridge, which is SE of the Plateau. An issue for examining deformation in the inner recess is the presence and geometry of these transitions in the Plateau.

Workers agree that the Plateau in the recess was an area of active blind thrusting during the late Paleozoic formation of the central Appalachian portion of the Alleghanian thrust belt (Gwinn, 1964; Kulander and Dean, 1986; Wilson and Shumaker, 1992). Blind thrust flats transferred displacement into the Plateau from the belt, forming the Browns Mountain anticline (BMA) above a duplex and also, several detachment folds with central Appalachian trends (Fig 8). In contrast, most workers (Kulander and Dean, 1986; Woodward, 1985; Whitaker and Bartholomew, 1999) do not believe that displacement from the southern Appalachian portion of the Alleghanian thrust belt was transferred into the Plateau. Instead, up to 20 km of thrust displacement for the southern Appalachian St. Clair thrust sheet emerges through the surface trace of the St. Clair thrust in front of the Plateau (Fig. 5a). Using this pair of interpretations, thin-skinned penetrative deformation in the Plateau should only be related to central Appalachian shortening because a blind flat was only operative in this area at that time.

An alternative hypothesis (Fig. 5b) is that the St. Clair thrust is only an imbricate fault of a blind thrust flat, which continues into the Plateau (Couzens and Dunne, 1994). If true, thin-skinned penetrative deformation could occur in this area throughout development of the Alleghanian thrust belt because a blind thrust flat was operative at all times. In this case, the Plateau could have experienced either continuous or episodic deformation during blind thrust accommodation for both the formation of the southern and central Appalachian portions of the Alleghanian thrust belt. Continuity of behavior may also indicate that the blind Wills Mountain duplex of the central Appalachians is laterally continuous with the St. Clair thrust sheet of the southern Appalachians, which both have about 20 km of displacement (Wilson and Shumaker, 1992; Couzens and Dunne, 1994). Such an interpretation for recess development will be tested

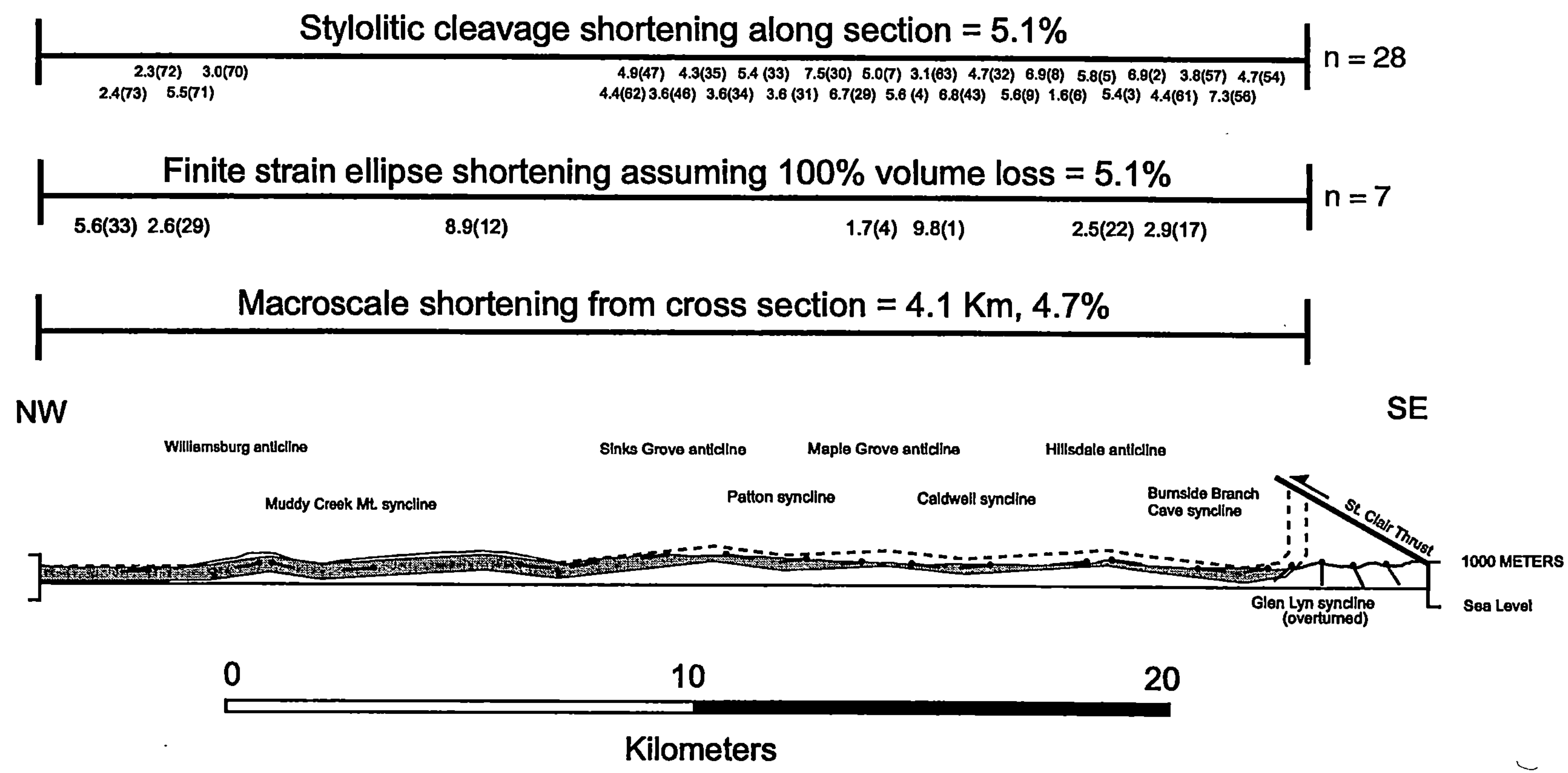

Fig. 8. Cross section of Mississippian Greenbrier Group (gray) shown with a thickness of 340 m (Reger and Price, 1926; Ogden, 1976; Skinner, 1979). Also shown are contributions to total shortening of submap-scale structures from measurements of cleavage and Fry analyses (station numbers are in parentheses next shortening percentages, see Table 4).

in this study by considering shortening magnitudes, directions and timings in the Plateau rocks. Shortening data will be presented as a function of scale.

3. Macroscale Shortening

A geologic cross section was constructed to estimate macroscale shortening for the Greenbrier Group in the Plateau beyond the St. Clair thrust (Figs. 4, 8). The cross section was constrained by using surface geologic contacts, structural geometries and stratigraphic thicknesses. Previous mapping in the area (Reger and Price, 1926; Ogden, 1976; Skinner, 1979) supplemented structural and stratigraphic data from this study. The cross-section line was positioned in the center of the recess near the termination of map-scale central and southern Appalachian folds, which should be an area with relatively little map-scale shortening. The section was constructed along 150-330°; which is normal to the southern Appalachian structural trend so as to be able to integrate the shortening contribution of smaller structures in this direction. This integration will allow the issue of the timing and magnitudes of shortening components to be examined. Not all structures along this section are of southern Appalachian origin or geometry, although, the section is being used to resolve shortening components parallel to a normal to the southern Appalachian trend and is not an attempt at a restoration or "balancing".

The transect crosses 11 folds from the overturned Glenn Lyn syncline in the SE to the Williamsburg anticline in the NW. The folds are shown as open folds with straight limbs and constant layer-normal thickness, based on field observations of fold shapes and preservation of layer thickness through folds (Fig. 8). Also, map-scale faults are absent from the Greenbrier Group in the cross section as they were not found during mapping in the study area.

The component of macroscale shortening parallel to the section within the Greenbrier Group was measured as a line length change (Dahlstrom, 1969), because bed thicknesses are preserved in rock exposures. An initial bed length of 28.3 km and a final bed length of 27 km yields 1.3 km or 4.7% macroscale section-parallel shortening by a combination of folds with central and southern Appalachian trends (18% southern and 82% central).

4. Strain Assessment

4.1. Greenbrier Cleavage Shortening

Limestones of the Mississippian Greenbrier Group are well exposed throughout the study area (Figs. 4, 9). Outcrop-scale folds and faults are almost completely absent in the Greenbrier Group. Instead, the dominant outcrop-scale structure is cleavage (Dean et al., 1988).

Cleavage morphology within the Greenbrier Group is dependent on lithology. Cleavage in wackestones and mudstones (Dunham, 1962) is typically smooth and parallel but sometimes anastomosing (Powell, 1979). Packstones have smooth to stylolitc cleavage. Grainstones commonly have stylolitic cleavage. Cleavage truncates bedding laminations, and clay is preferentially concentrated in the cleavage zones. Bedding-cleavage intersection angles

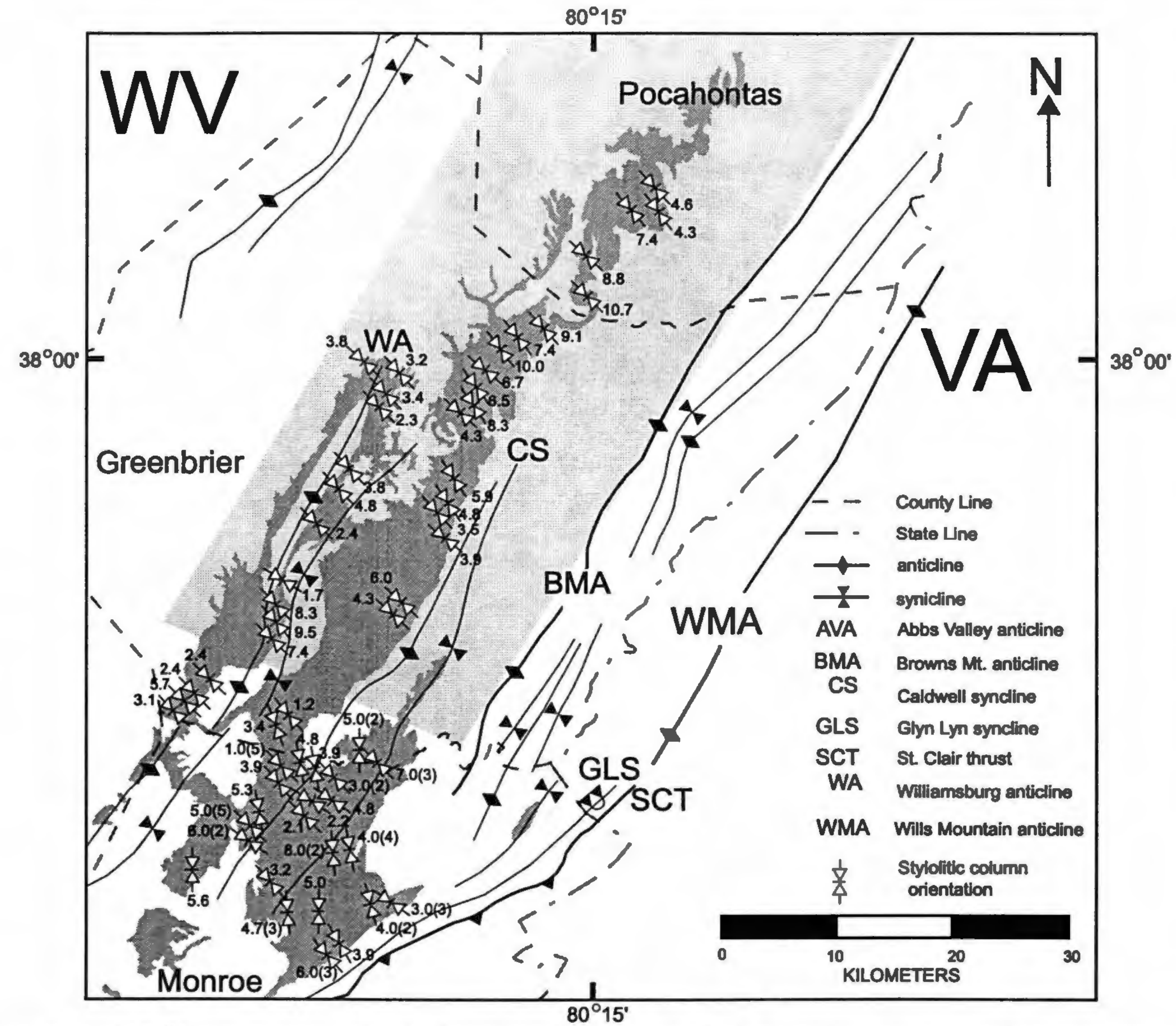

Fig. 9. Map showing stylolitic column orientations and estimated shortening magnitudes across cleavage. Number in parentheses is number of sample sites for an average value. Greenbrier outcrop shown in dark gray, transitional domain shown in white, and northern domain shown in medium gray. Total Sample population = 92.

typically exceed 85°, indicating a bed-normal geometry, which implies that cleavage was near vertical if formed while bedding was horizontal. Previous work (Dean et al., 1988) identified a complex array of multiple layer-parallel shortening directions from stylolitic column geometries across the region (Fig. 10). These workers did not identify the relative ages of the shortening directions on the basis of crosscutting cleavage geometries, nor did they estimate shortening magnitudes. As a result, the grainstones and packstones with stylolitic cleavage were re-examined to: (1) review the number and array of layer-parallel shortening directions; (2) determine relative age of shortening directions from crosscutting relationships; and (3) estimate shortening magnitudes from column amplitudes (Smart et al., 1997).

Shortening magnitude estimates for the cleavage were obtained from scanlines parallel to the stylolite teeth orientation on bedding, because this trend represents the actual shortening direction (Fig. 11). A minimum of three scanline measurements was taken for each station as a test for consistency. Shortening was calculated as an elongation (Means, 1976, p.135) where the final length is the length of the scanline and the initial length is the final length plus the sum of the stylolite amplitudes. This technique assumes that the amplitude of the stylolite teeth represents the width of dissolved material, which is a minimum estimate of shortening because volume loss could have occurred without increasing stylolite amplitude (Geiser and Sansone, 1981). This assumption of minimum shortening is a premise of the original solution explanation for stylolite

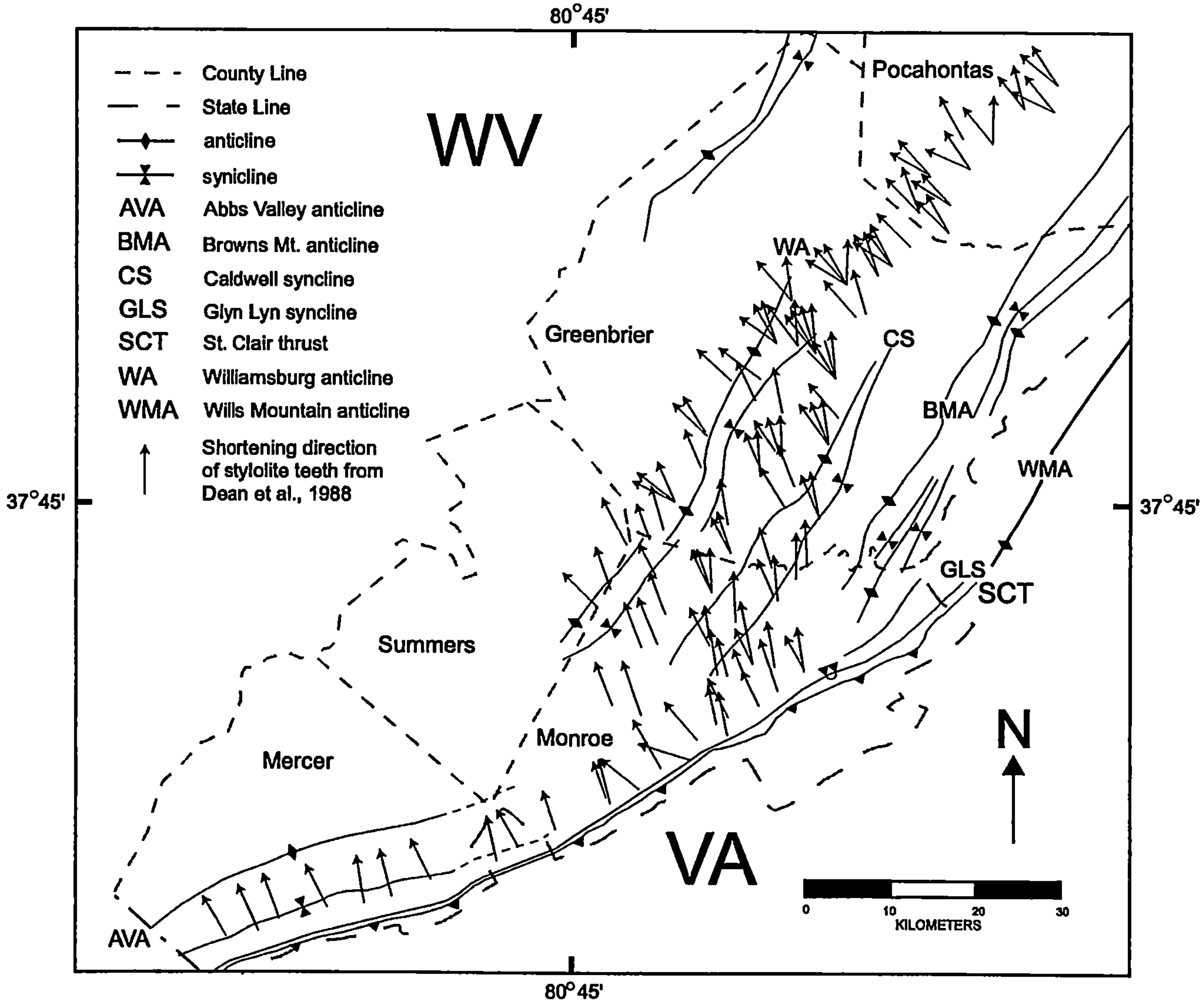

Fig. 10. Stylolitic cleavage shortening directions modified from Dean et al.(1988).

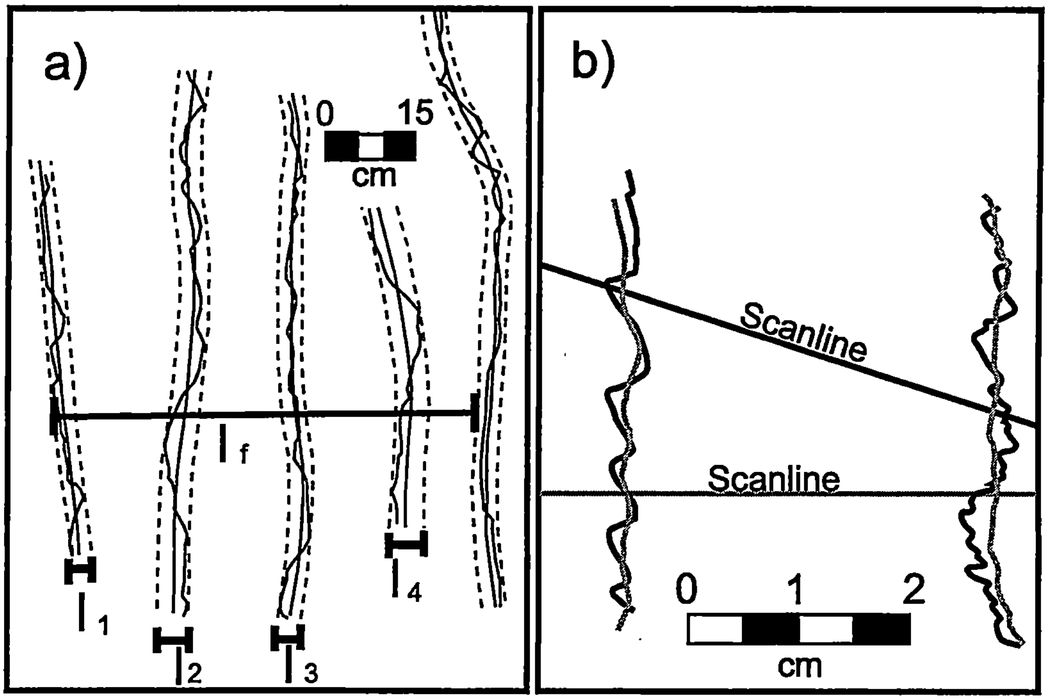

$$l_i = l_f + l_1 + l_2 + l_3 + l_4$$

Fig. 11. (a) Schematic representation of shortening measurements from stylolitic cleavage traces on a bedding surface. (b) Scanlines oriented parallel to stylolite column orientation (black - older traces, gray - younger traces).

formation (Stockdale, 1922, p. 59), is an explicit result of stylolite formation as anticracks (Fletcher and Pollard, 1981), and is consistent with an independent measure of strain versus size of teeth (Alvarez et al., 1978).

Based on the results to be presented in this paper, I divided the Plateau in the Roanoke recess into three structural domains (Fig. 12). The domains also have internally consistent macrostructural characteristics. The southern domain contains only structures with a southern Appalachian trend. The transitional domain contains folds with a central Appalachian trend at 030° but is bound to the southeast by a fold and thrust with a southern Appalachian trend. The northern domain contains only folds with central Appalachian trends.

Four stylolitic-column measurements from the southern domain show shortening oriented from 319° to 330°, subnormal to the host southern Appalachian folds, with an average of 324° ± 5° (Table 1, Fig. 12). Shortening magnitudes range from 3.5% to 5.7%, averaging 4.3% ± 1%.

59 cleavage measurements from the transitional domain were parsed into three groups of similar shortening directions (Table 1, Fig. 9). No measured shortening directions lie in the range of 290° to 300°, which would be expected if a true central Appalachian shortening direction were recorded. Instead, 66% (39 measurements) of the data lie between 300° and 320°, which is intermediate in orientation to between the southern and central shortening directions. These data average a trend of 313° ± 6° with shortening magnitudes of 0.6% to 8.3% that average 4.4 ± 2%. Only three measurements indicated shortening oriented

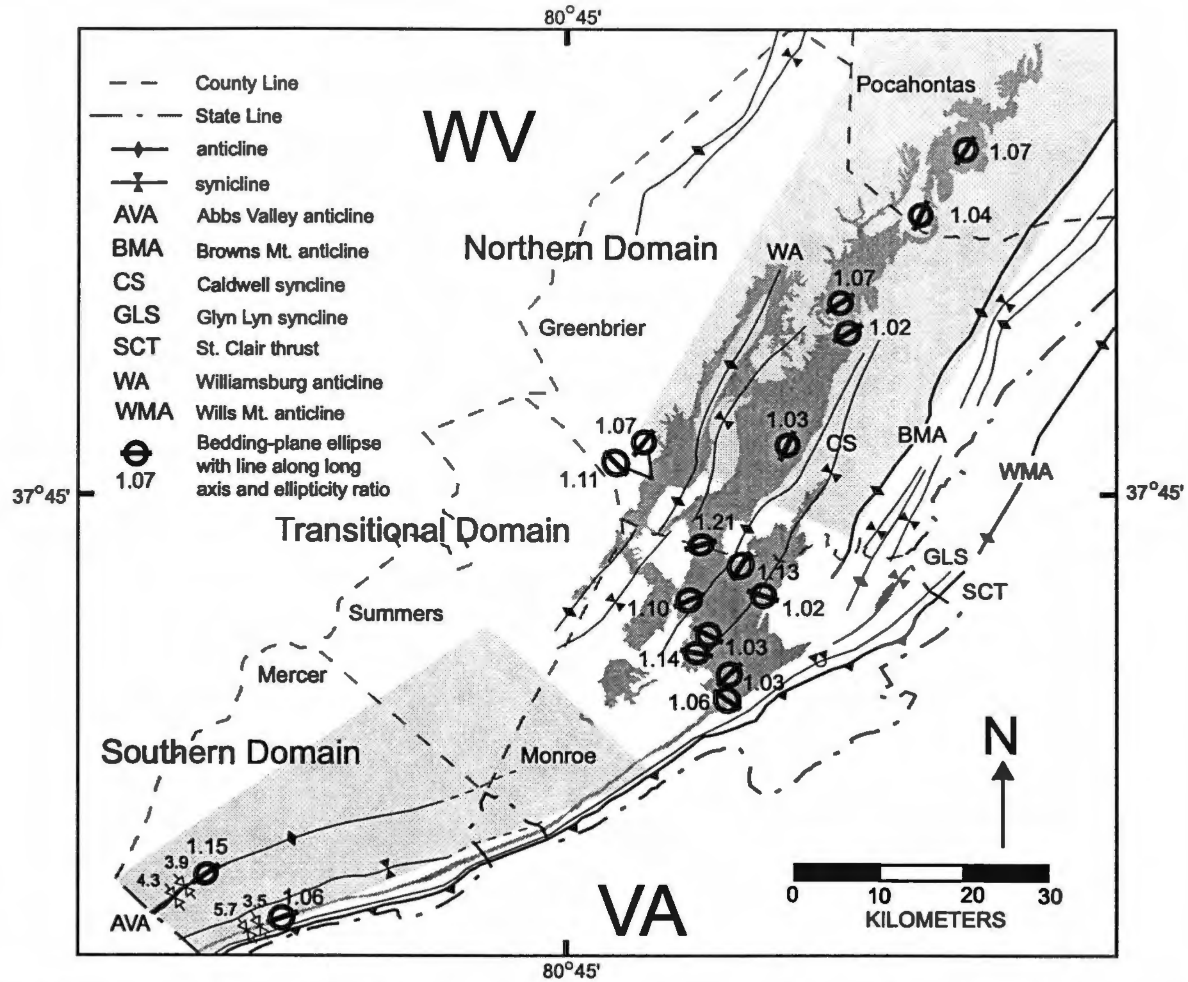

Fig. 12. Map showing bedding-plane strain ellipses calculated from normalized Fry method (Fry, 1979; Erslev, 1988) and cleavage shortening values of the southern domain. Medium gray used to show northern and southern structural domains while the transitional domain is unornamented. Outcrop of Greenbrier Group in dark gray. Total number of samples = 17.

Table 1. Stylolitic cleavage data

Stylolitic Cleavage Data For Southern Domain

Station Number	Bedding Orientation	Cleavage Unrotated*	Cleavage Rotated**	Teeth Orientation	Number of Traces	Average Column Amplitude (cm)	Scanline Length (cm)	Percent Shortening
113	057/60	065/30	053/90	323°	6	1	100	5.7
114	060/62	059/25	060/87	330°	6	0.6	100	3.5
115	059/60	070/23	055/83	325°	9	0.5	100	4.3
116	059/60	078/33	229/88	319°	5	0.8	100	3.8
Average:				324° ± 5°				4.3 ± 1%

Stylolitic Cleavage Data For Transitional Domain With Shortening Oriented 300-320

Station Number	Bedding Orientation	Cleavage Unrotated*	Cleavage Rotated**	Teeth Orientation	Number of Traces	Average Column Amplitude (cm)	Scanline Length (cm)	Percent Shortening
1	051/09	221/82	222/81	312°	13	0.35	50	8.3
2	159/13	037/90	218/83	308°	10	0.8	100	7.4
3	161/06	041/83	041/86	311°	10	0.6	100	5.7
5	162/08	214/88	214/83	304°	14	0.5	100	6.5
6	174/03	047/87	047/89	317°	5	0.2	60	1.6
8	184/09	052/78	051/84	320°	5	0.3	20	7
9	180/08	050/82	049/87	319°	6	0.5	50	5.7
22	029/03	213/82	213/85	303°	8	0.1	35	2.2
23	033/05	215/80	215/85	305°	5	0.5	50	4.8
24	308/07	044/80	045/81	315°	4	0.4	75	2.1
32	115/07	228/86	228/89	318°	4	1	80	4.8
36	222/14	032/90	032/90	302°	10	0.3	80	3.6
37	122/10	034/82	033/82	303°	3	1	60	4.8
38	122/10	038/84	037/83	307°	2	1.5	50	5.7
39	210/16	038/70	038/86	308°	13	1	200	6.1
40	215/18	036/82	216/80	306°	6	1	100	5.7
41	030/28	210/79	030/73	300°	4	0.4	50	3.1
42	068/16	038/68	040/82	310°	3	0.3	50	1.8
43	198/18	048/80	228/84	318°	3	1	40	7
48	216/08	045/84	225/88	315°	9	1	100	8.3
49	205/05	050/82	050/87	320°	10	0.8	100	7.4
52	044/10	224/82	044/88	314°	11	0.5	100	5.2
54	255/06	048/65	049/70	319°	3	1	60	4.8
55	245/05	045/70	046/75	316°	9	0.8	100	6.7
56	248/06	048/72	049/78	319°	8	1	100	7.4
63	225/20	045/80	225/80	315°	2	0.5	30	3.2
66	238/20	225/66	226/86	316°	4	0.5	60	3.2
67	240/20	225/74	222/55	312°	6	0.4	50	4.6
70	209/23	225/76	045/82	315°	4	0.4	50	3.1
71	030/03	045/90	045/90	315°	2	0.3	10	5.7
72	028/16	227/78	047/87	317°	5	0.3	60	2.4
73	184/06	050/90	230/86	320°	2	0.5	40	2.4
83	040/05	045/90	045/85	315°	3	0.8	60	3.8
84	048/17	047/73	047/90	317°	2	0.4	40	2
86	194/18	082/90	263/83	315°	1	0.6	60	1
88	158/19	082/90	081/85	320°	1	0.6	60	1
90	026/06	080/90	080/86	320°	1	0.6	100	0.6
92	066/06	080/90	080/84	320°	1	0.6	100	0.6
93	240/08	040/90	220/82	310°	7	0.5	100	3.4
Average:				313° ± 6°				4.4 ± 2%

Stylolitic Cleavage Data For Transitional Domain With Shortening Oriented 330-340

Station Number	Bedding Orientation	Cleavage Unrotated*	Cleavage Rotated**	Teeth Orientation	Number of Traces	Average Column Amplitude (cm)	Scanline Length (cm)	Percent Shortening
4	161/06	215/90	215/86	340°	12	0.5	100	5.7
57	255/06	060/80	060/86	330°	4	0.5	50	3.8
89	026/06	222/73	222/79	340°	5	0.8	100	3.8
Average:				337° ± 6°				4.5 ± 1%

Stylolitic Cleavage Data For Transitional Domain With Shortening Oriented 341-360

Station Number	Bedding Orientation	Cleavage Unrotated*	Cleavage Rotated**	Teeth Orientation	Number of Traces	Average Column Amplitude (cm)	Scanline Length (cm)	Percent Shortening
7	184/09	122/86	121/82	350°	5	0.5	45	5.3
16	155/07	035/87	215/89	345°	6	0.5	50	5.7
21	145/22	042/81	040/86	344°	6	0.3	90	2
29	226/13	037/78	217/89	355°	8	1	100	7.4
30	226/13	037/78	217/89	355°	9	1	100	8.3
31	066/07	038/90	038/90	350°	5	0.8	100	3.8
33	060/05	040/90	040/90	350°	6	1	100	5.7
34	060/05	045/90	045/90	350°	5	0.8	100	3.8
35	060/05	045/90	045/90	350°	6	0.8	100	4.6
46	264/14	040/86	220/84	360°	3	1	70	4.1
47	198/10	054/90	054/90	360°	3	1.2	60	5.7
61	054/06	044/90	044/84	360°	2	0.8	30	5.1
62	260/11	046/90	226/81	355°	4	0.5	40	4.8
85	194/18	224/74	043/90	354°	3	0.8	60	3.8
87	158/19	043/90	224/82	355°	3	1	60	4.8
91	066/06	222/83	222/88	350°	4	1	100	3.8
94	240/08	087/90	267/83	357°	2	0.6	100	1.2
Average:				353° ± 5°				4.7 ± 2%

Stylolitic Cleavage Data For Northern Domain With Shortening Oriented 300-330

Station Number	Bedding Orientation	Cleavage Unrotated*	Orientation Rotated**	Teeth Orientation	Number of Traces	Average Column Amplitude (cm)	Scanline Length (cm)	Percent Shortening
10	214/51	210/33	212/84	302°	3	0.2	35	1.7
12	210/11	226/83	227/72	317°	9	0.5	50	8.3
13	202/03	050/83	050/86	320°	7	0.6	40	9.5
15	200/10	045/80	045/89	315°	8	1	100	7.4
74	038/10	226/78	226/88	316°	5	0.3	60	2.4
76	010/16	047/69	045/82	315°	5	0.8	80	4.8
77	022/18	049/74	048/90	318°	4	0.8	80	3.8
78	028/05	048/90	048/85	318°	7	0.2	40	3.4
79	018/09	046/90	046/82	316°	3	0.4	50	2.3
80	016/12	048/62	045/72	315°	2	0.5	30	3.2
81	240/10	222/72	043/82	313°	2	1	50	3.8
95	355/04	225/78	224/81	330°	9	0.5	100	4.3
96	355/04	080/90	080/90	330°	8	0.8	100	6
97	200/04	042/78	042/82	312°	9	0.5	100	4.3
98	210/06	056/82	056/87	326°	6	1.5	100	8.3
99	210/08	054/80	054/87	324°	7	1	100	6.5
100	205/05	040/80	040/85	310°	6	1.2	100	6.7
101	204/06	054/75	053/80	323°	8	1.4	100	10.1
102	200/06	052/61	052/86	320°	8	1	100	7.4
103	208/05	048/84	048/89	330°	10	1	100	9.1
104	205/05	045/78	045/83	315°	5	1.2	50	10.7
105	210/08	042/80	042/88	312°	6	0.8	50	8.8
106	204/06	050/84	050/89	320°	8	1	100	7.4
107	200/05	048/82	048/86	318°	6	0.8	100	4.6
108	200/09	054/82	054/89	324°	9	0.5	100	4.3
109	206/05	055/78	055/82	325°	7	0.9	100	5.9
110	206/05	046/76	046/81	316°	5	0.5	50	4.8
111	202/06	042/75	042/81	312°	6	0.6	100	3.5
112	208/10	038/79	038/89	308°	5	0.8	100	3.8
Average:				318° ± 7°				5.8 ± 3%

* Indicates orientation with bedding.
** Indicates orientation after bedding is rotated to horizontal.

from 321° to 340°, which would contain the typical southern Appalachian shortening direction and so are a statistically minor group. Instead, the remaining twenty-nine percent (17 measurements) of the data indicate shortening oriented more northerly than the typical southern Appalachian shortening direction. These data average a trend of 353° ± 5° with shortening magnitudes of 1.2 to 7.4% that average 4.7 ± 2%.

29 cleavage measurements from the northern domain (Table 1, Fig. 9) all have shortening trends (300°-330°) that are intermediate between the central Appalachian shortening direction (295°-300°) and the southern Appalachian shortening direction (325°-330°). Fifty-nine percent (17 measurements) of the data fall between 310° and 320°, and overall, the 29 measurements average a trend of 318° ± 7°. Shortening magnitudes range from 1.7% to 10.7% with an average of 5.8 ± 3%.

As recognized by Dean et al. (1988) (Fig. 10), the stylolitic cleavage shows a more complex array of shortening directions as compared to the simpler set of trends for the map-scale structures. However, I found the complexity to be focused only in the transitional zone, unlike Dean et al. (1988). Stylolites in the southern domain are consistently parallel with the map-scale folds and faults of the southern Appalachians. The dominant shortening directions recorded by the stylolites in the transitional domain are not normal to the trends of either central or southern Appalachian map-scale structures. Instead, they are parallel to an intermediate 317° and an almost N-S trend of 353°. I found the stylolitic cleavage of the northern domain to record only one dominant shortening trend of 318°, which is not normal to map-scale structures. This simplicity of trend distribution contrasts with the results of Dean et al. (1988) (Fig. 9, 10). In terms of magnitudes, shortening is typically about 4.5% for the southern and transitional domains (Table 1), but increases to the northern domain with an average of 5.8% and a weak NE gradient of increasing strain magnitude in that domain.

4.1.2. Crosscutting cleavage

Given the variety of shortening directions recorded by stylolites in the transitional domain, determining their age relationships would ideally be achieved by comparing the different stylolites and teeth orientations at the same exposure. As it turns out, the only relative age data come from examining a single set of stylolites that has the unusual morphology of teeth overprinting teeth. Evidence for a deformation sequence for shortening directions is obtained for crosscutting stylolitic columns along the same cleavage surfaces. Seven oriented samples were collected of stylolite surfaces trending 042°-050° with this morphology (Figs. 13, 14). The samples were cut into slabs and polished to reveal and verify the morphology, as it is very difficult to identify in the field (Figs. 6b, 13). The first set of asymmetric columns is much more noticeable with a thick clay selvage and shortening magnitudes averaging around 3.5% with a column trend of 342° ± 9°. In all cases, sinuous traces of the second set of teeth

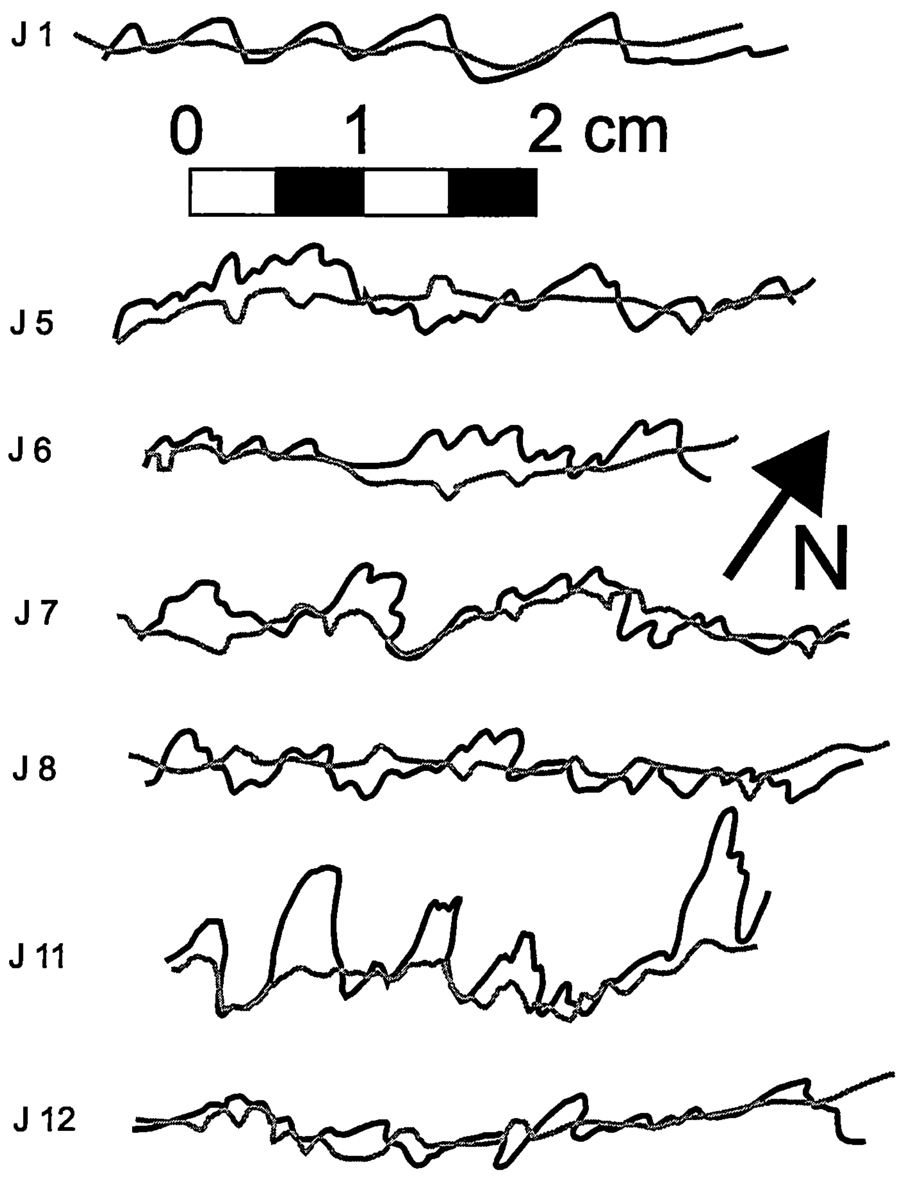

Fig. 13. Diagram example of cross-cutting stylolitic cleavage morphologies from seven oriented samples. The black lines represent the first cleavage and gray lines are the second cleavage.

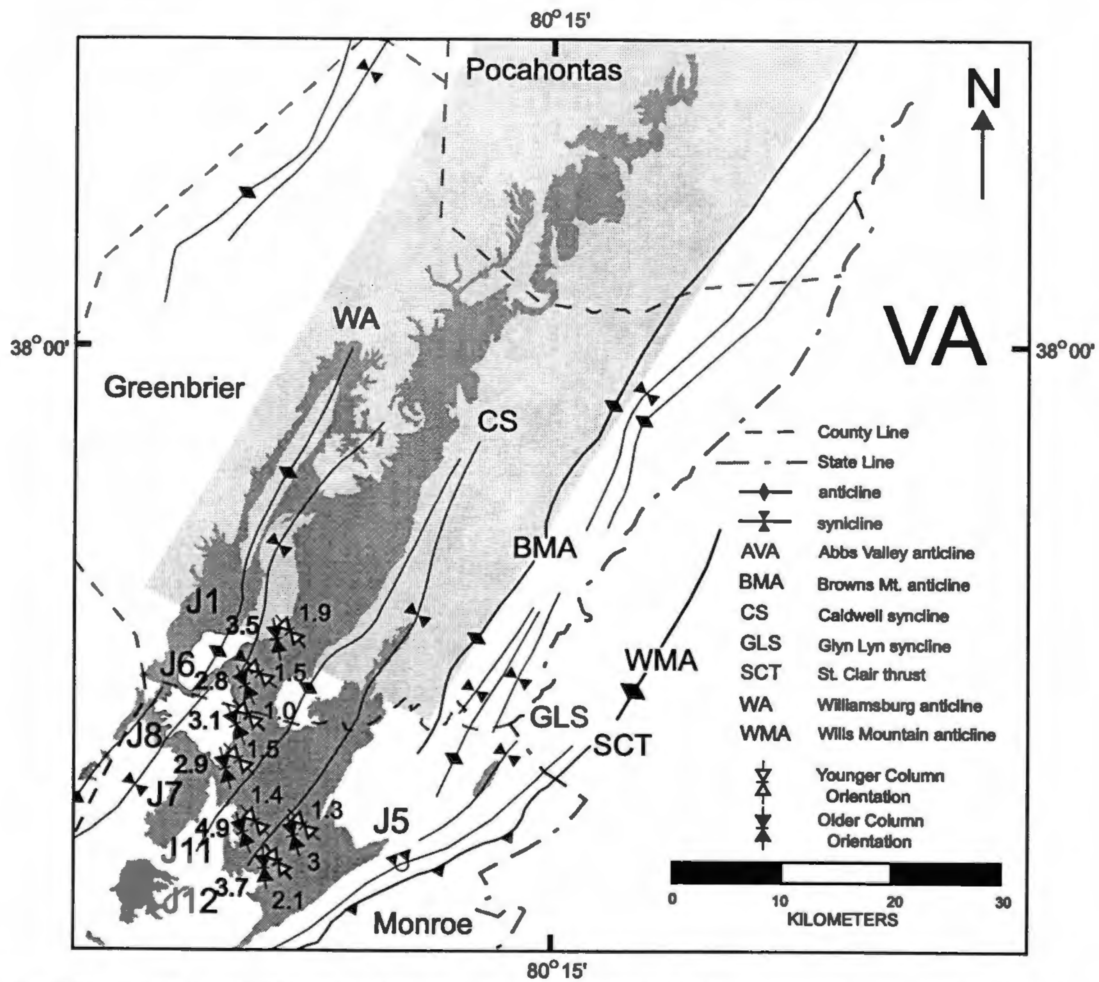

Fig. 13. Map showing difference in shortening directions and estimated shortening magnitudes for sample locations with crosscutting stylolitic teeth. Greenbrier outcrop in dark gray, transitional domain in white, and northern domain in medium gray. J values are station numbers (see Figure 12). Total number of stations = 7.

cut through the first set and hence, are younger. The second set of more symmetric columns has less clay and a smaller shortening magnitude averaging less than 2% with a column trend of 322° ± 4°. Crosscutting relationships indicate that the northerly shortening direction is older than the shortening direction that is intermediate to the central and southern Appalachian shortening directions.

Also, sets of stylolitic cleavage trending 060°-075° and 030°-045° are present in the same outcrops in the transitional domain. Dean et al. (1988) interpreted these sets to result from coaxial deformation by the stylolitization of pre-existing joint surfaces. I also found both sets to have only one orientation for teeth of 350°-360°, indicating that they are the same age (Dean et al., 1988; Smart et al., 1997).

4.2. Calcite Twins

The calcite strain-gauge technique was used to calculate twinning strains in about 25 grains from each of two mutually perpendicular sections for 12 samples (Figs. 6c, 15, Table 2). Calculations used the inner twin width for thick twins and a twinned material ratio of 0.5 for thin twins (Groshong, 1972; 1974; Groshong et al., 1984a; Evans and Groshong, 1994). Measurement precision and accuracy were improved by discarding 20% of the twin sets with the largest deviation from the calculated strain tensor, minimizing measurement errors (Groshong, 1974; Groshong et al., 1984a; 1984b; Ferrill, 1991; Ferrill and

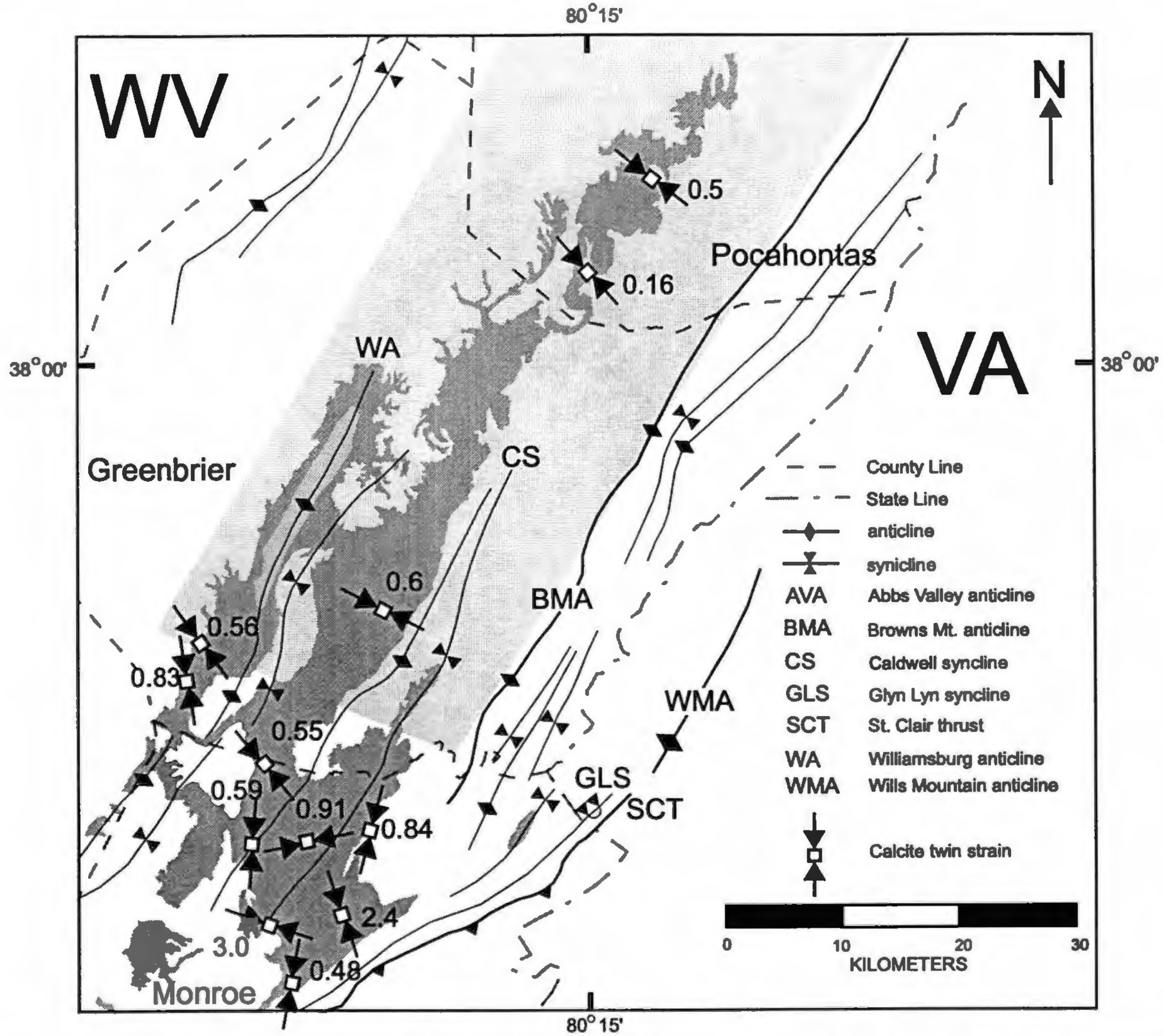

Fig. 15. Map showing calcite twin-strain magnitudes and shortening directions in the transitional and northern domains. Total number of samples = 12.

Table 2. Calcite twin data.

Sample Number Bedding	Cleaning procedure*	Number of twin sets	Principal Strains (% elongation) e1	e2	e3	Principal axis orientations** e1	e2	e3	Nominal error in strain	Percent NEV	Average twin width (mm)	Average twin intensity (twin/mm)	Total distortion (% strain)
1	n.a.	50	5.9	-1	-4.9	337/83	119/05	209/4	0.88	12	0.67	94	5.40
010/12NW	LDR	40	2.3	1.2	-3.5	307/71	120/18	210/2	0.48	17.5	0.56	82	3.10
3	n.a.	49	2.9	0.3	-3.2	251/75	70/15	160/00	0.37	20.4	0.69	59	3.10
034/24NW	LDR	40	2.3	0.2	-2.5	253/62	072/28	162/00	0.34	10	0.56	55	2.40
9	n.a.	50	1.1	-0.1	-1	062/28	197/54	320/22	0.2	22	0.32	44	1.10
030/58NW	LDR	40	0.5	0	-0.5	063/38	213/48	321/15	0.09	12.5	0.17	39	0.60
11	n.a.	50	1.4	0.2	-1.6	167/79	341/11	071/01	0.17	36	0.38	50	1.50
058/20NW	LDR	40	0.8	0.2	-1	143/81	350/08	259/04	0.17	25	0.27	46	0.90
12	n.a.	49	0.6	0.4	-1	269/76	092/14	002/01	0.34	26.5	0.29	61	0.90
159/13SW	LDR	40	0.5	0.1	-0.6	283/61	091/28	185/07	0.15	37.5	0.16	55	0.60
17	n.a.	50	1.5	0.2	-1.7	139/05	246/75	047/14	0.33	8	0.29	77	1.60
046/14SE	LDR	40	0.9	0	-0.9	146/12	268/69	049/16	0.11	7.5	0.17	69	0.90
21	n.a.	49	1.2	0.1	-1.3	079/87	286/12	196/01	0.19	28.6	0.29	52	1.20
108/07NE	LDR	40	0.7	0.2	-0.9	059/83	285/05	195/05	0.09	22.5	0.17	49	0.80
22	n.a.	49	1	0.4	-1.4	112/73	283/16	013/03	0.16	4.1	0.27	66	1.20
046/16SE	LDR	40	0.4	0.1	-0.5	103/16	266/73	011/05	0.07	0	0.14	58	0.50
29	n.a.	50	0.9	0.3	-1.2	058/66	270/21	175/12	0.27	30	0.27	65	1.10
134/20SW	LDR	40	0.4	0.2	-0.6	067/45	276/41	172/15	0.1	20	0.14	63	0.60
33	n.a.	50	1.5	-0.2	-1.3	283/69	060/15	154/13	0.25	24	0.27	71	1.40
136/20SW	LDR	40	0.9	-0.2	-0.7	271/61	048/22	145/18	0.11	25	0.15	65	0.80
A1	n.a.	50	0.4	-0.2	-0.2	048/83	188/06	279/05	0.07	18	0.37	12	0.30
025/06W	LDR	40	0.18	-0.07	-0.11	067/84	229/06	319/01	0.03	22.5	0.21	11	0.16
A6	n.a.	50	0.9	-0.1	-0.8	199/68	41/21	308/08	0.12	34	0.3	37	0.80
020/06W	LDR	40	0.5	0	-0.5	208/63	35/27	304/02	0.05	27.5	0.16	34	0.50
A7	n.a.	50	1.3	0.2	-1.5	045/40	188/45	298/19	0.57	34	0.42	40	1.40
024/07W	LDR	40	0.5	0.2	-0.7	042/48	201/40	300/10	0.13	30	0.23	36	0.60

*LDR, 20% of largest deviations removed; n.a., not applicable
** with bedding horizontal

Groshong, 1993a; b).

The total distortion for twinned samples varies from 0.16% to 3.03%, and averages 0.96 ± 0.86%, but if the two samples with much larger strains are removed (1 and 3, Table 2), the average is 0.61 ± 0.22%. This second average is more representative of the other 10 samples, which have total distortions that are only 5% to 40% of the two larger strains. Distortion magnitudes are quite comparable to magnitudes determined from twins in the Greenbrier Group samples gathered to the north about 70 kilometers where the rocks only record central Appalachian deformation (Smart et al., 1997).

In the northern domain, the three twin samples have an average shortening direction (e_3 axial directions) of 308° ± 10° (Fig. 14, Table 2). This trend is subnormal to the axes of folds with central Appalachian trend and subparallel to the shortening direction of 318° ± 7° as determined from the columns of the stylolitic cleavage.

The transitional domain contains three distinct populations of orientations for e_3 axes (Fig. 15, Table 2). Five samples have an approximately N-S trend of 009° ± 23°, two samples have essentially an E-W trend, and two samples have a NW-SE trend. The calcite twins record the same complexity of shortening directions (e_3 directions) in the transitional domain that were interpreted from the columns of the stylolitic cleavage samples in this domain (Table 1, 2; Figs. 9, 14, 15). N-S shortening (5 samples) and NW-SE shortening (3 samples), which are oblique to both the southern and central Appalachian shortening directions, are present. In addition, the twins record a nearly E-W shortening direction (2 samples) that is absent in the measured cleavage data, but was locally recorded by Dean et al. (1988) in this domain.

As strain recorders for a specific deformation mechanism, twins record very small deformations for low temperatures, stresses and differential stresses (Burkhard, 1993). They also record orogenic deformation well beyond the limits of a thrust belt (Craddock and van der Pluijm, 1989). So, different twins in the same sample could record components of both southern and central Appalachian shortening (Groshong, 1972; 1974; Burkhard, 1993). If so, these components might be parsed out by separating negative expected values (NEV) from positive expected values (PEV) for each sample set of twins. When e_3 axes are plotted for the twin samples from this study area for the NEV populations of the samples, they show no clear pattern (Fig. 16). This results is perhaps not surprising as the NEV's are measurements that least fit the calculated ellipsoid for the entire sample population of twins, rather than having a characteristic shortening direction or magnitude. Given that these twin measurements are collected in an area with a known noncoaxial history, this result supports the reservations of Burkhard (1993) about attempting to parse different shortening events from calcite twins, using filters such as NEV's.

4.3. Fry Analyses

Three mutually perpendicular thin sections were prepared from each of 17 oriented ooid grainstone samples for application of the normalized Fry method

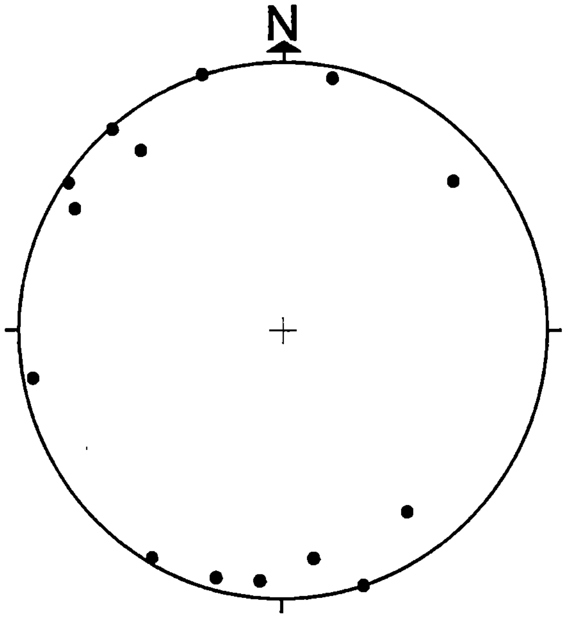

Fig. 15. Equal-area lower hemisphere projection of calcite twin short (e_3) axes with bedding rotated to the horizontal.

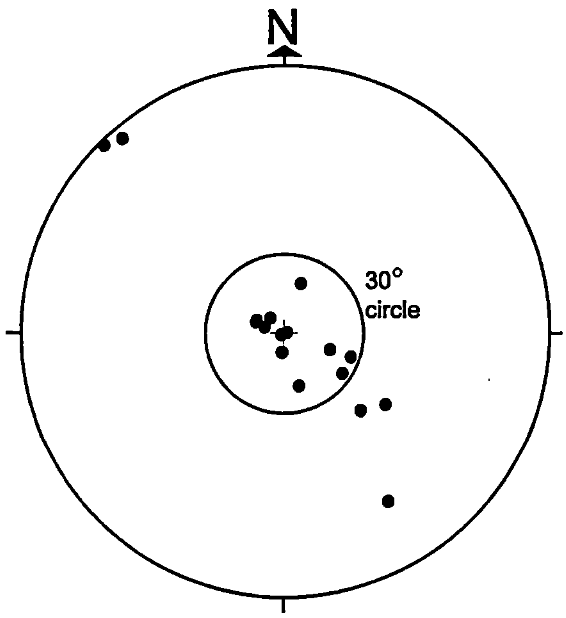

Fig. 16. Equal-area lower hemisphere projection of principal strain ellipsoid short (Z) axes determined by normalized Fry method with bedding rotated to the horizontal.

(Fry, 1979; Erslev, 1988). Enlarged photomicrographs of each thin section were digitized for ooid grain boundaries using software developed by W. A. Yonkee (pers. Comm.). Finite strain ellipses were determined from measurements of 250 ooid grain boundaries for each section and finite strain ellipsoids were calculated for each sample (Owens, 1984).

The strains were measured in rock volumes between the outcrop-scale stylolites but where twins are present. Consequently, these strains record the effects of deformation in the stylolite microlithons and include calcite-twin strains (Fig 6c). Ideally, the shortening measured for the stylolitic cleavage and shortening magnitudes from the R values of the strain ellipses from the normalized Fry measurements could be added to characterize the total strain from cleavage development and internal microlithon deformation.

Principal shorten (Z) axes for the strain ellipsoids are nearly bed-normal in 14 of 17 samples, while the Z axes are nearly bed-parallel in 2 of the other 3 samples (Fig. 17). Bedding-perpendicular thin-sections from all the samples exhibit bedding-parallel transgranular pressure-solution seams and sutured grain boundaries indicative of pretectonic vertical compaction, which is consistent with the geometry of the Z-axes. Assuming that pretectonic compaction was a uniaxial flattening with the short axis of the strain ellipsoid normal to bedding, bedding-parallel strain ellipses would be circular after compaction. Thus, thin-sections oriented parallel to bedding were analyzed to measure layer-parallel strain (LPS) that followed the compactional event.

The southern domain contains 2 samples with short ellipse axes that are

Table 3. Finite strain ellipsoid calculations

Input Sample Number	Orientation	Plane	Strike	Dip	Rake	R	Output Axis	Stretch	Axis Trend	Axis Plunge	Rxy	Ryz	Rxz	Solution Used	Axis Trend*	Axis Plunge
S1	010/12 NW	b	190	12	89	1.14	z	0 92	125	76	1.11	1.08	1.2	Q33	185	84
		p	10	78	4	1.1	y	1	10	6					9	6
		v	280	90	13	1.17	x	1.11	279	13					279	1
S4	024/24NW	b	204	7	92	1.03	z	0.88	111	68	1.04	1.14	1.18	Q33	110	75
		p	24	83	179	1.13	y	1	204	1					204	1
		v	294	90	23	1.18	x	1.04	295	22					295	15
S9	030/58NW	b	212	58	137	1.21	z	0.92	126	34	1.21	1.09	1.32	Q33	110	68
		p	32	32	2.5	1.21	y	1	246	37					204	1
		v	302	90	58	1.17	x	1.21	8	35					295	22
S12	159/13SW	b	159	13	88	1.1	z	0.9	69	77	1.06	1.11	1.18	Q33	90	89
		p	339	77	0	1.14	y	1	335	1					335	0
		v	249	90	14	1.14	x	1.06	244	13					244	0
S13	048/17SE	b	48	17	163	1.14	z	0.86	117	67	1.06	1.17	1.24	Q33	125	51
		p	228	73	4	1.13	y	1	282	22					276	35
		v	318	90	17	1.19	x	1.06	14	5					16	14
S17	046/14SE	b	46	14	1	1.03	z	0.91	135	70	1	1.1	1.1	Q33	135	56
		p	226	76	1	1.07	y	1	1015	10					18	17
		v	316	90	20	1.1	x	1	282	17					279	28
S21	108/07NE	b	288	7	59	1.05	z	0.83	20	81	1.11	1.21	1.33	Q33	19	74
		p	108	83	1	1.17	y	1	278	2					278	3
		v	198	90	7	1.35	x	1.11	188	9					188	16
S22	046/16SE	b	46	16	125	1.06	z	0.89	103	83	1.07	1.13	1.21	Q33	125	68
		p	226	74	0	1.2	y	1	284	7					282	20
		v	316	90	16	1.12	x	1.07	194	0					15	8
S23	065/08NW	b	245	8	152	1.02	z	0.95	193	87	1.02	1.06	1.08	Q33	317	84
		p	65	82	1.5	1.07	y	1	306	1					126	6
		v	335	90	3	1.06	x	1.02	36	3					216	1
S28	070/08NW	b	250	8	169	1.07	z	1	320	12	1.05	1	1.05	Q33	320	5
		p	70	82	178	1.02	y	1	152	77					140	85
		v	340	90	8	1.02	x	1.05	50	3					50	0
S29	134/20SW	b	134	20	1	1.11	z	0.92	44	71	1.05	1.08	1.14	Q33	224	89
		p	314	70	0	1.08	y	1	228	19					48	1
		v	224	90	21	1.13	x	1.05	137	1					137	0
S30	069/66SE	b	69	66	92	1.07	z	0.94	337	41	1.03	1.06	1.09	Q33	164	73
		p	249	24	178	1.09	y	1	75	8					259	2
		v	336	90	157	1.05	x	1.03	174	48					350	17
S32	058/29NW	b	238	29	179	1.02	z	0.92	328	3	1.01	1.09	1.1	Q33	148	26
		p	58	61	0	1.1	y	1	125	86					332	65
		v	328	90	106	1.15	x	1.01	238	1					239	1
S33	136/20SW	b	136	20	90	1.07	z	0.97	317	2	1.07	1.04	1.11	Q33	316	2
		p	316	70	91	1.07	y	1	49	38					51	58
		v	226	90	42	1.08	x	1.07	225	52					225	32
A1	025/06NW	b	205	6	0	1.03	z	0.87	191	89	1.04	1.15	1.2	Q33	285	84
		p	25	84	1	1.2	y	1	296	0					116	6
		v	295	90	0	1.15	x	1.04	26	1					26	1
A6	020/06NW	b	200	6	1	1.07	z	0.92	292	87	1.04	1.09	1.13	Q33	291	81
		p	20	84	0	1.1	y	1	113	3					113	9
		v	290	90	0	1.11	x	1.04	23	0					23	0
A7	024/7NW	b	204	7	91	1	z	0.89	295	88	1.03	1.12	1.16	Q33	294	81
		p	24	83	0	1.09	y	1	203	0					202	0
		v	294	90	0	1.18	x	1.03	113	2					112	9

* Bedding horizontal.

locally normal to the axes of their host folds (Table 3, Fig. 12). The ellipticities (R) of the bed-parallel ellipses are 1.06 and 1.15.

The transitional domain, consisting of ten samples, again has a complex pattern of shortening directions as interpreted from the trends of the short axes of the bedding-parallel strain ellipses (Table 3, Fig. 12). Five ellipses have short axes with a N to NE trend, that is nearly strike-parallel, ranging from 11° to 45° with an average of 27° ± 13° (Table 3). These samples have R values from 1.02 to 1.14 with an average of 1.07 ± 0.05. Another three ellipses have short axes with trends oblique to southern and central Appalachian shortening directions with orientations ranging from 301° to 317° and R values from 1.03 to 1.14. The two remaining ellipses have short axes with a NNW trend of 337° and 345°, and R values of 1.10 and 1.21, respectively.

Five samples from the northern domain have a bimodal pattern of short axes trends (Table 3, Fig. 12). Three samples have short axes normal to map-scale central Appalachian axial traces with an average of 298° ± 5°, and low R values of 1.03 to 1.07. The two remaining samples have short axes oriented at 327° and 329° with small R values of 1.02 and 1.07, respectively.

4.3.1. Magnitude of LPS as a function of volume loss

Interpreting ellipticity ratios (R) as a measure of strain is a function of understanding deformation mechanisms (Ramsay and Huber, 1983; Groshong, 1988). A key issue for low-temperature deformation of limestone is the role of

Table 4. Fry analyses bedding plane ellipse data.

Southern Domain

Southern Appalachian Trend

Sample Number	R	Volume Loss	Trend*
30	1.06	-6%	341
32	1.15	-13%	325

Northern Domain

Southern Appalachian Trend

Sample Number	R	Volume Loss	Trend*
23	1.02	-2%	327
28	1.07	-6%	329

Central Appalachian Trend

Sample Number	R	Volume Loss	Trend*
a1	1.04	-3%	295
a6	1.07	-6%	303
a7	1.03	-3%	295

* Bedding restored to the horizontal.

Transitional Domain

Strike-Parallel Trend

Sample Number	R	Volume Loss	Trend*
1	1.14	-13%	11
4	1.03	-3%	26
21	1.02	-2%	18
22	1.06	-6%	35
29	1.11	-10%	45

NW-NNW Trend

Sample Number	R	Volume Loss	Trend*
9	1.21	-17%	345
12	1.10	-9%	337

WNW-NW Trend

Sample Number	R	Volume Loss	Trend*
13	1.14	-12%	301
17	1.03	-3%	317
33	1.07	-6%	308

dissolution mechanisms (Groshong, 1976). For example with plane strain, a 100% volume-loss deformation requires much greater shortening to achieve the same R value than a volume-constant deformation because the elongation is a function of R rather than the square root of R (Ramsay and Huber, 1983). For the grainstones and packstones of the Greenbrier Group, grain-to-grain sutures and transgranular stylolites are abundant in thin section and handspecimen, whereas twins, the only structures from constant volume deformation, account for only very small strains (Table 2, Fig. 14). Consequently, R values for the strain ellipses in bedding were treated as being a result of volume loss. Assuming plane strain because of the lack of extension structures, elongations were calculated (Table 3). Shortening magnitudes range from 2 to 17% with the smallest overall strains occurring in the northern domain.

5. Discussion

5.1 Spatial distribution of shortening directions

For the southern domain, short axes of strain ellipses, stylolitic columns and the trend of map-scale structures are all consistent with the simple interpretation that they resulted from a single southern Appalachian shortening event on the southwest flank of the Roanoke recess. For the northern domain, interpreted shortening directions record a slightly more complex deformation history. Twins and Fry plots indicate shortening directions subnormal to the trends of the central Appalachian folds, whereas stylolitic cleavage records an average shortening direction of 318° ± 7° that is oblique to both southern and central Appalachian shortening directions. As the cleavage is contained in the limbs of the central Appalachian folds, I agree with Dean et al. (1988) that the cleavage is the older structure. Interestingly, the shortening magnitude of the stylolites is greater in this domain, whereas the twins and Fry plots record relatively smaller strains as compared to the other two domains. Thus, the northeastern flank of the Roanoke recess records an earlier NW-directed shortening in the stylolitic cleavage that is overprinted by shortening of a central Appalachian trend that is recorded by map-scale folds, and twins and grain-scale solution structures that account for the strain measured with the Fry method.

The transitional domain is the true center for complex smaller-scale deformation in the study area. The stylolitic cleavage, twins and Fry plots locally record a near N-S shortening trend, which is the oldest shortening direction recorded by the cleavage in the domain. Again, all indicators record a NW-SE shortening trend that is oblique to both southern and central Appalachian shortening directions, although, the magnitude of shortening decreases to the southwest from the northern into the transitional domain. Only twins and a few stylolites found by Dean et al. (1988, p. 309) locally record an E-W shortening trend, which Dean et al. (1988) incompletely argued to be the youngest stylolites in the area. Also, only the grain-scale solution structures locally record shortening parallel to the trend of the central Appalachian folds as measured by the Fry method. Thus, in the transitional domain, shortening directions are recorded over an arc of greater than 90°, although smaller scale indicators do not record shortening trends specifically parallel to the southern and central Appalachian shortening directions.

Deformation is heterogeneously distributed in space in the domain (Fig. 9, 12, 15), indicating that locally, rocks only accommodated portions of the deformation. Given that deformation likely occurred at less than 200°C based on conodont color alteration indices of 2.0 to 3.0 from the Greenbrier Group (Epstein et al., 1977; Harris et al., 1978; Harris et al., 1994), this spatial heterogeneity probably reflects the fact that stylolitic columns, twins and grain-to-grain sutures are difficult structures to alter once emplaced when deformation is low-temperature, discontinuous and spatially heterogeneous (Groshong, 1976; 1988; Burkhard, 1993, Dunne & Caldanaro, 1997). For example, overprinting of stylolites in the study area required formation of a second set of solution surfaces rather than direct modification of the existing stylolitic columns (Fig. 13). Also, twins were seldom kinked by other twins, or bent by unseen dislocation-slip surfaces. The twins additionally show the typical intensities and sizes (Table 2) expected for low-temperature twinning, when nucleation of new twins dominates over twin widening (Ferrill, 1991).

In terms of deformation sequence in the transitional domain, all types of smaller-scale shortening indicators are folded in the limbs of central Appalachian folds (Dean et al., 1988), indicating that the folds are younger. Whitaker and Bartholomew (1999), however, found that smaller-scale structures recording the NW-SE shortening trend are preserved in the overturned limb of the Glen Lyn syncline, which is a southern Appalachian structure. As a result, the inner arc of the Roanoke recess records NW-SE shortening by smaller-scale structures preceding any larger-scale structures of either southern or central Appalachian origin. Smaller-scale deformation preceding larger-scale deformation is typical of low-temperature limestone deformation in foreland thrust belts (Marshak and Engelder, 1985; Craddock and van der Pluijm, 1989; Holl and Anastasio, 1995).

5.2. Evolution of the Roanoke Recess

Combining the new data about the distribution and timing of shortening with the existing observations that larger-scale structures deform smaller ones (Dean et al., 1988; Whitaker & Bartholomew, 1999) leads to a revised interpretation about the deformation sequence at this recess. The essence of this reinterpretation is that the deformation was continuous rather than two-step around the recess. Evidence for discounting a two-step deformation history includes:

(1) Overprinting of smaller-scale structures with common shortening directions by southern and central Appalachian map-scale structures that have different trends.

(2) Continuity of map-scale structures around the recess, such as the Staunton-Pulaski fault system or the anticline at the NE termination of the St. Clair thrust into the Wills Mountain anticline (Butts, 1933; Calver, 1963; Butts, 1973; Rodgers, 1970; Bartholomew, 1981; Bartholomew, 1987).

(3) Map-scale structures of these two trends do not produce interference

patterns, which would be expected for sequential overlapping map-scale structures. A possible exception was identified by Bick (1986), but has been descredited by Bartholomew (personal communication; Whitaker and Bartholomew, 1999).

The only surviving direct evidence for sequential deformation would be that central Appalachian structures deform younger rocks and that a few structures such as the Rich Patch anticline have an oblique structural trend at the intersection of the two trends (Rodgers, 1970). However, the age difference of the deformed rocks could be an artifact of erosional differences, and the oblique structures lack interference patterns and may represent a locally segmented rather than smoothly curving structural geometry around the recess.

Discarding a two-step interpretation for the deformation history of the recess, a new interpretation needs to incorporate the following observations:

(1) The deformation occurred at a pre-existing promontory (Thomas, 1977; Hatcher et al., 1989).

(2) Deformation along strike to the south of the recess records a coaxial deformation for all structures.

(3) Deformation to the north of the recess records a two-step sequence where outcrop-scale cleavage produced NW-directed shortening, followed by WNW-directed shortening by map-scale and microscale structures with a typical central Appalachian shortening direction (Dean et al., 1988).

(4) The NW-directed shortening by cleavage is found at the center and to the north of the recess. In the center, it is folded by map-scale southern

Appalachian structures (Whitaker and Bartholomew, 1999).

(5) The center of recess (transitional domain) records a series of deformation directions from oldest N-directed (stylolitic teeth) to NW-directed (stylolitic teeth) to NNW-directed and WNW-directed (map-scale structures) to W-directed (stylolitic teeth) with the last observation from Dean et al. (1988).

(6) In the center, the variety and ages of shortening directions do not have a spatial arrangement consistent with simple bending about the recess (Fig. 2 vs. Fig. 9, 12, 15).

I interpret these observations to represent a progressive deformation around a recess where the center of the deformation intensity migrates northeastward around the recess. I will present this interpretation as stages, but these stages are just a convenient means for illustrating the highlights of the deformation history as opposed to representing time discrete steps:

Stage 1: Deformation initiated to the south of the recess beginning the coaxial NNW-directed deformation there while at some point penetrating into the recess with N-S directed shortening.

Stage 2: Deformation continued in the south, and both the center of the recess and rocks to the north developed cleavage recording a NW-directed shortening event. A key question is why this new deformation was NW-directed rather than NNW-directed as it was to the south. The data do not contain the basis for a definitive answer, and I offer the possibility that the existence of the promontory caused a clockwise refraction of displacement directions.

Stage 3: Deformation continued with map-scale structures folding the cleavage in both the center of the recess and in rocks to the north. The map-scale structures changed from a southern Appalachian trend to a central Appalachian trend northeastward with a lack of overprinting and the presence of large laterally continuous structures. I interpret the lack of overprinting and the continuity as evidence for northeastward propagation of the map-scale structures as the deformation center migrated in the same direction. Deformation could have continued to the south during this time, but the data do not contain evidence to support or refute this contention.

Stage 4: The deformation center migrated around the recess so that deformation was then concentrated to the north of the recess, producing the late-stage, localized W-directed deformation recorded by cleavage in the recess center (Dean et al., 1988) and continued the WNW-directed deformation to the north at all scales. South of the recess lacks evidence for structural overprint at this stage, perhaps due to insufficient deformation intensity, or because for these low-temperature conditions, the available energy is insufficient for the task of deforming rocks that already contain thrusts, folds, cleavage and smaller-scale structures.

Considering the general models for salient development (Fig. 2)(e.g. Marshak, 1988; Hindle and Burkhard, 1999), they typically have "centers of deformation" such that the axis of maximum displacement for the finite deformation is coincident with the axes for incremental maximum displacement. Put differently, the displacement field evolves symmetrically with a fixed axis of maximum displacement that reflects an assumed continuity of boundary conditions and initial geometric characteristics (Macedo and Marshak, 1999; Hindell and Burkhard, 1999). In contrast, the Roanoke recess preserves a strain pattern that is asymmetric spatially and temporally. My interpretation hypothesizes that this asymmetry of the strain pattern is a result of asymmetry in the displacement pattern. I believe that the displacement pattern was asymmetric around the recess throughout Alleghanian deformation and that the axis of maximum displacement migrated NE through time. As a result, an attempt to classify my interpretation in terms of general models (orocline or primary arc) (Marshak, 1988; Hindle and Burkhard, 1999) will fail because the deformation pattern in the recess does not match the kinematic assumptions for the models.

It is still possible to consider primary causes for recess formation in terms of factors such as the presence of buttresses in the foreland, location of basinal depocenters or obiquity of plate convergence (Macedo and Marshak, 1999). In that context, the recess may be viewed as a pre-existing buttress that was not a depocenter. The key problem for this view is resolving the nature of the "center of deformation", which changed position outside the study area through time during deformation. At some level, the center is related to the mechanics of plate collision during the Alleghanian orogeny. It would be convenient for the center to represent the shifting focus of impact between Laurentia and Gondwanaland through time (Sacks and Secor, 1990; Geiser and Engelder, 1983), but my data is insufficient to validate this additional interpretation because they are only kinematic data derived from the perimeter of the orogenic belt.

Other possibilities exist such as segmentation of Gondwanaland by faults that changed indenter geometry or changing spatial distribution of the mechanical strength of the basal detachment beneath the orogen through time. Nonetheless, my interpretation shows that the Roanoke recess is not an intersection recess like the Kingston recess (Marshak and Tabor, 1989). Instead, deformation was continuous during a single orogenic event rather than episodic, and the displacement maximum migrated rather than being bimodal or stationary.

Comparing the proposed deformation history of the Roanoke recess to the Pennsylvania salient shows that these two tectonic features did not experience "mirror" deformations. The Pennsylvania salient records an orderly pattern of shortening directions rotating out from the center. In the center of the salient in the Juniata culmination, deformation is coaxial through time with shortening oriented between 322° and 340° (Nickelsen and Engelder, 1989; Spiker and Gray, 1997). A counterclockwise Alleghanian stress field rotation is indicated to the south (Nickelsen and Hough, 1967; Nickelsen, 1988; Evans, 1994) and a clockwise stress field rotation indicated to the north of this culmination (Nickelsen, 1979; Engelder and Geiser, 1980; Gray and Mitra, 1993; Younes and Engelder, 1999). Deformation appears to be active throughout the salient at all stages. In contrast, deformation progressed northeastward in the recess during an overall clockwise rotation of the shortening-direction from SW to NE. Thus, while the recess and salient may have formed in response to the same bulk plate tectonic behavior, they pursued unique deformation histories to achieve their present forms.

5.3. Existence of a Blind Detachment

The St. Clair fault, which has up to 20 km displacement, terminates in a regional anticline at the junction of the southern and central Appalachians. Couzens and Dunne (1994) suggested that this termination is the result of displacement transfer to a blind thrust instead of simply a displacement decrease to zero for an emergent thrust (Dahlstrom, 1969). This hypothesis would require up to 20 km of shortening to be accommodated by Plateau rocks above a proposed thrust flat that are to the foreland of the surface trace of the St. Clair fault.

Measurements of stylolite amplitudes allow a minimum estimate of shortening for the mesoscale cleavage, and bedding-plane finite strain ellipses allow an estimation of shortening within cleavage microlithons. Shortening magnitudes vary along the section (Table 5, Fig. 8), but show no systematic pattern that would necessitate data partitioning. Therefore, average values calculated for the strains across the cleavage zones and microlithons are added to the map-scale macroscale shortening estimate from the cross section to provide a more accurate estimate of total shortening (Dunne, 1996). To average the shortening magnitudes, each shortening vector must be resolved into its component along the 150°-330° section (Table 5). This calculation is possible for

Table 5. Corrected shortening values from data for stylolitic cleavage and for the normalized Fry method

Cleavage data

Station Number	Cleavage Rotated*	Teeth Orientation	Measured Shortening	Corrected Shortening along 330
54	049/70	319°	4.8	4.7
55	046/75	316°	6.7	6.5
56	049/78	319°	7.4	7.3
57	060/86	330°	3.8	3.8
61	044/84	360°	5.1	4.4
2	218/83	308°	7.4	6.9
3	041/86	311°	5.7	5.4
5	214/83	304°	6.5	5.8
6	047/89	317°	1.6	1.6
8	051/84	320°	7.0	6.9
9	049/87	319°	5.7	5.6
32	228/89	318°	4.8	4.7
43	228/84	318°	7.0	6.8
63	225/80	315°	3.2	3.1
4	215/86	340°	5.7	5.6
7	121/82	350°	5.3	5.0
29	217/89	355°	7.4	6.7
30	217/89	355°	8.3	7.5
31	038/90	350°	3.8	3.6
33	040/90	350°	5.7	5.4
34	045/90	350°	3.8	3.6
35	045/90	350°	4.6	4.3
46	220/84	360°	4.1	3.6
47	054/90	360°	5.7	4.9
62	226/81	355°	4.8	4.4
70	045/82	315°	3.1	3.0
71	045/90	315°	5.7	5.5
72	047/87	317°	2.4	2.3
73	230/86	320°	2.4	2.4
Average:			5.2% ± 1.7	4.9% ± 1.6

*Bedding rotated to the horizontal

Fry method

Sample Number	Ellipticity Ratio (R)	Trend**	Measured Shortening	Corrected Shorting along 330
17	1.03	317°	3.0	2.9
22	1.06	35°	6.0	2.5
1	1.14	11°	13.0	9.8
4	1.03	26°	3.0	1.7
12	1.1	337°	9.0	8.9
29	1.11	45°	10.0	2.6
33	1.07	308°	6.0	5.6
Average:			7.1% ± 4	4.9% ± 3

**Trend of shortening axis with bedding rotated to the horizontal these finite strains because their magnitudes are measured as a 100% volume loss mechanism, which each have unique shortening directions. So vector magnitudes along section are corrected by multiplying the cosine of the angular difference between trend of the section and measured elongation vector with the measured magnitude. Cleavage shortening magnitudes along this cross section slightly decrease toward the foreland, averaging 5.1% across the entire section. Shortening calculated from bedding ellipse ellipticity ratio to 5.1% assuming 100% volume loss, and shortening calculated from the map-scale folds equals 4.7%.

Using the initial bed length previously determined for the Greenbrier limestone of 28.3 km, the combined shortening percentage of 14.9% represents 4.4 km of shortening. Therefore, total shortening as resolved parallel to 330° almost exceeds 15% which is quite comparable to shortening magnitudes recorded to the north in the central Appalachians (Engelder and Engelder, 1977; Smart et al., 1997). This magnitude of shortening does necessitate a blind floor thrust beneath the study area that formed before or during the onset of the stylolitic cleavage with NW-oriented teeth (Engelder and Engelder, 1977). This 4.4 km of shortening is significantly less than the 20 km of displacement for the St. Clair thrust, so if displacement transfer occurred along a blind thrust flat beneath the St. Clair thrust, significant shortening would have to be present further into the foreland. For example, accommodation of 20 km of displacement would require deformation across 130 km of the Plateau at the same shortening magnitude (14.9%) as measured in the study area, or smaller magnitudes parsed out over a longer distance. It is worth noting that Craddock and van der Pluijm (1989) have measured 1 to 2% calcite-twin strains in the Michigan basin that they attributed to Appalachian deformation. Therefore, while it is likely that an Alleghanian blind thrust is under the Greenbrier Group rocks of the Plateau, it is not clear that this fault accommodated as much of the displacement of the St. Clair thrust sheet as envisioned by Couzens and Dunne (1994). I believe that the existence of this blind flat supports the interpretation that St. Clair thrust sheet and the thrust horse under the Wills Mountain anticline are one feature (Wilson and Shumaker, 1992; Couzens and Dunne, 1994).

6. Conclusions

(1) The inner arc of the Roanoke recess in the Appalachian Plateau records Alleghanian deformation from microscale to mapscale that displays shortening directions ranging over greater than 90° and a total percentage magnitude near 15%. This magnitude is quite comparable to shortening magnitudes recorded further to the north in the central Appalachians.

(2) The array of shortening directions and relative age of the structures are interpreted to be the result of the progressive northeastward migration of the center for deformation around a pre-existing promontory. The deformation pattern is asymmetric with a progressive counterclockwise rotation of the shortening direction through time that is not the mirror of the deformation pattern to the north in the Pennsylvania salient where

deformation is symmetric and shortening directions rotate progressively outward through time.

(3) The shortening magnitude of about 15% (locally 4.4 km of shortening) necessitates an underlying blind decollement. Yet, this blind flat has not locally accommodated the 20 km displacement of the adjacent St. Clair thrust sheet, so for such an accommodation to occur, additional deformation would need to be present further into the foreland. The existence of the blind fault supports an interpretation where the St. Clair thrust sheet and the blind Wills Mountain duplex to the NE are the same continuous structure, as they both would connect to the same blind thrust into the foreland.

REFERENCES

REFERENCES

Alvarez, W., Engelder, T., Geiser, P.A., 1978. Classification of solution cleavage in pelagic limestones. Geology 6, 263-266.

Bartholomew, M.J., 1981. Geology of the Roanoke and Stewartsville quadrangles, Virginia. Virginia Division of Mining Resources Publication 34.

Bartholomew, M.J., 1987. Structural evolution of the Pulaski thrust system, southwestern Virginia. Virginia Division of Mineral Resources 34.

Bick, K.F., 1986. Structure of the Sugarloaf Mountain area: intersecting trends on the northeast flank of the Roanoke reentrant, Virginia, In: Mcdowell, R.C., Glover, Lynne, III, Rodgers, John, Bambach, R.K., Gray, D.R., (Eds.) The Lowry Volume: Studies in Appalachian Geology, Virginia Polytechnic Institute and State University, Department of Geological Sciences, Memoir 3, 27-36.

Burkhard, M., 1993. Calcite twins, their geometry, appearance and significance as stress-strain markers and indicators of tectonic regime: A Review. Journal of Structural Geology 15, 351-358.

Butts, C., 1933. Geological Map of the Appalachian Valley in Virginia. Virginia Geological Survey, scale 1:250,000.

Butts, C., 1973. Geology of the Appalachian Valley in Virginia, Part 1: geologic text and illustrations. Virginia Division of Mineral Resources Bulletin 52.

Calver, J.L., 1963. Geologic Map of Virginia. Virginia Division of Mineral Resources, scale 1:500,000.

Cardwell, D.H., Erwin, R.B., Woodward, H.P., 1968. 1968 Geologic map of West Virginia. West Virginia Geological and Economic Survey, 1:250,000.

Carey, S.W., 1955. The orocline concept in geotectonics. Paper and Proceedings of the Royal Society of Tasmania 89, 255-289.

Choukroune, P., Auvray, B., Francheteau, J., Lepine, J.C., Arthaud, F., Bruns, J.P., Auzende, J.M., Sichler, B., Khobar, Y., 1986. Deformation and motion in the western Alpine arc, Tectonics 5, 215-226.

Cloos, E., 1947. Ooelite deformation in the South Mountain fold, Maryland. Geological Society of America Bulletin 58, 843-917.

Couzens, B.A., Dunne, W.M., 1994. Displacement transfer at thrust terminations: the Saltville thrust and Sinking Creek anticline, Virginia, U.S.A. Journal of Structural Geology 16, 781-793.

Craddock, J.P., van der Pluijm, B.A., 1989. Late Paleozoic deformation of the cratonic carbonate cover of eastern North America. Geology 17, 416-419.

Dahlstrom, C.D.A., 1969. Balanced cross-sections. Canadian Journal of Earth Sciences 6, 743-760.

Dean, S.L., Kulander, B.R., Skinner, J.M., 1988. Structural chronology of the Alleghanian orogeny in southeastern West Virginia. Geological Society of America Bulletin 100, 299-310.

Dunham, R.J., 1962. Classification of carbonate rocks according to depositional texture. Memoir - American Association of Petroleum Geologists, 108-121.
Dunne, W.M., Caldanaro, A.J., Jr., 1997. Evolution of solution structures in a deformed quartz arenite: geometric changes related to permeability changes. Journal of Structural Geology 19, 663-672.
Dunne, W.M., 1996. The role of macroscale thrusts in the deformation of the Alleghanian roof sequence in the central Appalachians: A re-evaluation. American Journal of Science 296, 549-575.
Engelder, T., Engelder, R., 1977. Fossil distortion and decollement tectonics of the Appalachian Plateau. Geology 5, 457-460.
Engelder T., Geiser, P.A., 1979. The relationship between pencil cleavage and lateral shortening within the Devonian section of the Appalachian Plateau, New York. Geology 7, 460-464.
Epstein, A.G., Epstein, J.B., Harris, L.D., 1978. Conodont color alteration—an index to organic metamorphism. United States Geologic Survey Professional Paper 995, 27p.
Erslev, E.A., 1988. Normalized center-to-center strain analysis of packed aggregates. Journal of Structural Geology 10, 201-209.
Evans, M.A., Groshong, R.H., Jr., 1994. A computer program for the calcite strain-gauge technique. Journal of Structural Geology 16, 277-281.
Evans, M.A., 1994. Joints and decollement zones in Middle Devonian shales: Evidence for multiple deformation events in the Central Appalachian Plateau. Geological Society of America Bulletin 106, 447-460.
Ferrill, D.A., Groshong, R.H., Jr., 1993a. Kinematic model for the curvature of the northern Subalpine Chain, France. Journal of Structural Geology 15, 523-541.
Ferrill, D.A., Groshong, R.H., Jr., 1993b. Deformation conditions in the northern Subalpine Chain, France, estimated from deformation modes in coarse-grained limestone. Journal of Structural Geology 15, 995-1006.
Ferrill, D.A., 1991. Calcite twin widths and intensities as metamorphic indicators in natural low-temperature deformation of limestone. Journal of Structural Geology 13, 667-675.
Fletcher, R.C., Pollard, D.D., 1981. Anticrack model for pressure solution surfaces. Geology 9, 419-424.
Fry, N., 1979. Random point distributions and strain measurement in rock. Tectonophysics 60, 89-105.
Geiser, P.A., Engelder, T., 1983. The distribution of layer parallel shortening fabrics in the Appalachian foreland of New York and Pennsylvania: Evidence for two noncoaxial phases of Allaghanian orogeny. In: Hatcher, R.D., Jr., Williams, H., Zeitz, I. (Eds.), Contributions to the Tectonics and Geophysics of Mountain Chains. Geological Society of America Memoir 158, 161-175.
Geiser, P.A., Sansone, S., 1981. Joints, microfractures, and the formation of solution cleavage in limestone. Geology 9, 280-285.

Geissman, J.W., Callian, J.T., Oldow, J.S., Humphries, S.E., 1984. Paleomagnetic assessment of oroflexural deformation in west-central Nevada and significance for emplacement of allochthonous assemblages. Tectonics 3, 179-200.
Globerman, B.R., Coe, R.S., 1984. Discordant declinations from "in place" Upper Cretaceous volcanics, SW Alaska: Evidence for oroclinal bending? Abstracts with Programs -Geological Society of America, 16, 286.
Gray, M.B., Mitra, G., 1993. Migration of deformation fronts during progressive deformation: Evidence from detailed structural studies in the Pennsylvania Anthracite region, U.S.A. Journal of Structural Geology 15, 435-449.
Gray, M.B., Stamatakos, J., 1997. New model for evolution of fold and thrust belt curvature based on integrated structural and paleomagnetic results from the Pennsylvania salient. Geology 25, 1067-1070.
Groshong, R.H., Jr., Teufel, L.W., Gasteiger, C., 1984a. Precision and accuracy of the calcite strain-gage technique. Geological Society of America Bulletin 95, 357-363.
Groshong, R.H., Jr., Pfiffner, O.A., Pringle, L.R., 1984b. Strain partitioning in the Helvetic thrust belt of eastern Switzerland from the leading edge to the internal zone. Journal of Structural Geology 6, 5-18.
Groshong, R.H., Jr., 1972. Strain calculated from twinning in calcite. Geological Society of America Bulletin 83, 2025-2038.
Groshong, R.H., Jr., 1974. Experimental test of least-squares strain gage calculation using twinned calcite. Geological Society of America Bulletin 86, 1855-1864.
Groshong, R.H. 1976. Strain and pressure solution in the Martinsburg Slate, Delaware Water Gap, New Jersey. American Journal of Science 276, 1131-1146.
Groshong, R.H., Jr., 1988. Low-temperature deformation mechanisms and their interpretation. Geological Society of America Bulletin 100, 1329-1360.
Gwinn, V.E., 1964. Thin-skinned tectonics in the Plateau and northwestern Valley and Ridge provinces of the central Appalachians. Geological Sociey of America Bulletin 75, 863-900.
Harris, A.G., Harris, L.D., Epstein, J.B., 1978. Oil and gas data from Paleozoic rocks in the Appalachian basin: Maps for assessing hydrocarbon potential and thermal maturity (conodont color alteration isograds and overburden isopachs). US Geological Survey Miscellaneous Investigation Series I-917-E, scale 1:2,500,000.
Harris, A.G., Stamm, N.R., Weary, D.G., Repetski, J.E., Stamm, R.G., Parker, R.A., 1994. Conodont color alteration index (CAI) map and conodont-based age determinations for the Winchester 30' x 60' quadrangle and adjacent area, Virginia, West Virginia, and Maryland. US Geological Survey Miscellaneous Field Studies Map MF-2239, scale 1:100,000.

Hatcher, R.D., Jr., Thomas, W.A., Geiser, P.A., Snoke, A.W., Mosher, S., Wiltschko, D.W., 1989. Alleghanian orogen. In: Hatcher, R.D., Jr., Thomas, W.A., Viele, G.W. (Eds.), The Appalachian-Ouachita Orogen in the United States. Geological Society of America, The Geology of North America F-2, 233-318.
Hindle, D., Burkhard, M., 1999. Strain, displacement and rotation associated with the formation of curvature in fold belts; the example of the Jura Arc. In: Evans, J.P., Treagus, S.H. (Eds.), Questions in structural geology; 20th anniversary special issue. Journal of Structural Geology 21, 1089-1101.
Holl J.E., Anastasio, D.J., 1995. Cleavage development within a foreland fold and thrust belt, southern Pyrenees, Spain. Journal of Structural Geology 17, 357-369.
Kellogg, K.S., 1980. Paleomagnetic evidence for oroclinal bending of the southern Antarctic Peninsula. Geological Society of America Bulletin 91, I 414-I 420.
Kulander, B.R., Dean, S.L., 1986. Structure and tectonics of central and southern Appalachian Valley and Ridge and Plateau Provinces, West Virginia and Virginia. American Association of Petroleum Geologists Bulletin 70, 1674-1684.
Macedo, J., Marshak, S., 1999. Controls on the geometry of fold-thrust belt salients. Geological Society of America Bulletin 111, in press.
Marshak, S., Engelder, T., 1985. Development of cleavage in limestones of a fold-thrust belt in eastern New York. In: Hancock, P.L., Powell, C. McA. (Eds.), Multiple deformation in ductile and brittle rocks. Journal of Structural Geology 7, 345-359.
Marshak, S., Floettman, T., 1996. Structure and origin of the Fleurieu and Nackara arcs in the Adelaide fold-thrust belt, South Australia; salient and recess development in the Delamerian Orogen. Journal of Structural Geology 18, 891-908.
Marshak, S., Tabor, J.R., 1989. Structure of the Kingston Orocline in the Appalachian fold-thrust belt, New York. Geological Society of America Bulletin 101, 683-701.
Marshak, S., 1988. Kinematics of orocline and arc formation in thin-skinned orogens. Tectonics 7, 73-86.
Means, W.D., 1976. Stress and Strain: Basic Concepts in Continuum Mechanics for Geologists. Springer-Verlag, New York.
Meyer, T.J., Dunne, W.M., 1990. Deformation of Helderberg limestones above the blind thrust system of the Central Appalachians. Journal of Geology 98, 108-117.
Muehlberger, W.R., 1992. The tectonic map of North America, Southeast Sheet. American Association of Petroleum Geologists, scale 1:5,000,000.
Nickelsen, R.P., Engelder, T., 1989. Day 4; Fold-thrust geometries of the Juniata Culmination, Central Appalachians of Pennsylvania. In: Hanshaw, P.M. (Ed.), Metamorphism and tectonics of eastern and central North America; Volume 2, Structures of the Appalachian foreland fold-thrust belt. American Geophysical Union, 35-43.

Nickelsen, R.P., Hough, V.N.D., 1967. Jointing in the Appalachian Plateau of Pennsylvania. Geological Society of America Bulletin 78, 609-629.
Nickelsen, R.P., 1979. Sequence of structural stages of the Alleghany Orogeny, at the Bear Valley strip mine, Shamokin, Pennsylvania. American Journal of Science 279, 225-271.
Nickelsen, R.P., 1988. Structural evolution of folded thrusts and duplexes on a first-order anticlinorium in the Valley and Ridge Province of Pennsylvania. In: Mitra, G., Wojtal, S.F. (Eds.), Geometries and mechanism of thrusting, with special reference to the Appalachians. Special Paper-Geological Society of America 222, 89-106.
Ogden, A.E., 1976, The Hydrogeology of the central Monroe County Karst, West Virginia. Ph.D. thesis, West Virginia University, Morgantown.
Owens, W.H., 1984. The calculation of a best-fit ellipsoid from elliptical sections on arbitrarily oriented planes. Journal of Structural Geology 6, 571-578.
Perry, W.J., 1978. Sequential deformation in the central Apalachians. American Journal of Science 278, 518-542.
Powell, C.McA., 1979. A morphological classification of rock cleavage. Tectonophysics 58, 21-34.
Price, P.H., 1929. Pocahontas County. West Virginia Geological Survey, 501p., 2 maps.
Price, P.H., Heck, E.T., 1939. Greenbrier County. West Virginia Geological and Economic Survey, 846p., 2 maps.
Protzman, G.M., Mitra, G., 1990. Strain fabric associated with the Meade thrust sheet: implications for cross-section balancing. Journal of Structural Geology 12, 403-417.
Ramsay, J.G., Huber, M.I., 1983. The Techniques of Modern Structural Geology Volume 1: Strain Analysis. Academic Press, San Diego.
Reger, D.B., Price, P.H., 1926. Mercer, Monroe and Summers Counties. West Virginia Geological Survey, 963p., 3 maps.
Ries, A.C., Shackleton, R.M., 1976. Patterns of strain variation in arcuate fold belts. Philosophical Transactions of the Royal Society of London, Series A: Mathematical and Physical Sciences 283, 281-288.
Rodgers, J., 1970. The Tectonics of the Appalachians. John Wiley and Sons, New York.
Sacks, P.E., Secor, D.T., 1990. Kinematics of Late Paleozoic continental collision between Laurentia and Gondwana.
Schmid, S.M., Panozzo, R., Bauer, S., 1987. Simple shear experiments on cacite rocks; rheology and microfabric. In: Cobbold, P.R., Gapais, D., Treagus, S.H. (Eds.), Shear criteria in rocks. Journal of Structural Geology 9, 747-748.
Schwartz, S.Y., Van der Voo, R., 1983. Paleomagnetic evaluation of the orocline hypothesis in the Central and Southern Appalachians. Geophysical Research Letters 10, 505-508.
Skinner, J.M., 1979. A paleostress analysis of the Greenbrier Group, (Mississippian), Monroe County, West Virginia. M.S. thesis, University of Toledo.

Smart, K.J., Dunne, W.M., Krieg, R.D., 1997. Roof sequence response to emplacement of the Wills Mountain duplex: the roles of forethrusting and scales of deformation. Journal of Structural Geology 19, 1443-1459.
Spiker, E.C., Gray, M.B., 1997. A study of progressive deformation at the Allegheny Front, Lycoming County, PA. Abstracts with Programs - Geological Society of America 29, 82.
Stockdale, P.B., 1922. Stylolites: their nature and origin. Indiana University Studies 55.
Thomas, W.A., 1977. Evolution of Appalachian-Ouachita salients and recesses from reentrants and promontories in the continental margin. American Journal of Science 277, 1233-1278.
Whitaker, A.E., Bartholomew, M.J., 1999. Layer Parallel Shortening: A mechansim for determining deformation timing at the junction of the central and southern Appalachians. American Journal of Science 299, 238-254.
Wilson, T.H., Shumaker, R.C., 1992. Broad Top thrust sheet: an extensive blind thrust in the central Appalachians. American Association of Petroleum Geologists Bulletin 76, 1310-1324.
Woodward, N.B., 1985. Valley and Ridge thrust timing; critical evidence. Abstracts with Programs - Geological Society of America 17, 143.
Younes, A.I., Engelder, T., 1999. Fringe cracks; key structures for the interpretation of the progressive Alleghanian deformation of the Appalachian Plateau. Geological Society of America Bulletin 111, 219-239.

VITA

Steven Alan Spraggins was born in Huntsville, Alabama on April 19, 1973. After living in Aberdeen, Maryland, Killeen, Texas and Denison, Texas, he graduated from Russellville Senior High School in Russellville, Arkansas in June 1991. He received a Bachelor of Science Degree in Geology from the University of Arkansas in Little Rock in January, 1996. In August 1996, he enrolled in the graduate program at The University of Tennessee in Knoxville. The Master of Science Degree in Geology was received December, 1999.

He is presently working on remote sensing projects and providing space shuttle mission operation support as a scientist with the NASA Office of Earth Science at Johnson Space Center.